

運輸省港湾技術研究所

港湾技術研究所 報告

REPORT OF
THE PORT AND HARBOUR RESEARCH
INSTITUTE

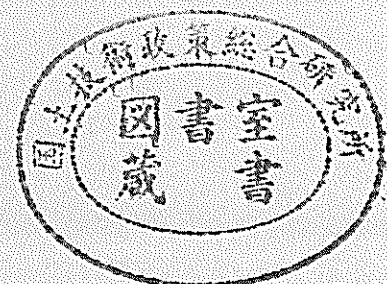
MINISTRY OF TRANSPORT

VOL.37

NO.4

Dec. 1998

NAGASE, YOKOSUKA, JAPAN



港湾技術研究所報告 (REPORT OF P.H.R.I.)

第 37 卷 第 4 号 (Vol.37, No.4) , 1998年12月 (Dec. 1998)

目 次 (CONTENTS)

1. Applicability of Dual Face Serpent-type Wave Generator
..... Tetsuya HIRAISHI, Katsuya HIRAYAMA, Haruhiro MARUYAMA..... 3
(デュアル・フェース・サーペント型造波装置の適用性
..... 平石 哲也・平山 克也・丸山 晴広)
2. Low-Frequency Ship Motions Due to Long-Period Waves in Harbors, and
Modifications to Mooring Systems That Inhibit Such Motions
..... Satoru SHIRAISHI..... 37
(長周期波による係留船舶の長周期動揺と係留システムによる動揺低減対策
..... 白石 悟)
3. Performance of the Quay Walls with High Seismic Resistance
..... Koji ICHII, Susumu IAI, Toshikazu MORITA..... 79
(耐震強化岸壁の耐震性能に関する有効応力解析
..... 一井 康二・井合 進・森田 年一)
4. 内湾域における泥質物の堆積過程に関する研究
..... 中川 康之..... 113
(A Study on Sedimentation of Mud in a Bay
..... Yasuyuki NAKAGAWA)
5. サクション基礎沈設時の必要排水量に関する考察
..... 善 功企・山崎浩之・森川嘉之・小池二三勝..... 135
(Study on Drainage Volume Necessary for Penetration of Suction Foundation
..... Kouki ZEN, Hiroyuki YAMAZAKI, Yoshiyuki MORIKAWA, Fumikatsu KOIKE)
6. 海洋環境下における再生コンクリートの適用性に関する研究
..... 伊藤正憲・福手 勤・田中 順・山路 徹..... 149
(A Study on Applicability of Recycled Concrete to Marine Structures
..... Masanori ITO, Tsutomu FUKUTE, Jun TANAKA, Toru YAMAJI)

Performance of the Quay Walls with High Seismic Resistance

Koji ICHII*
Susumu IAI**
Toshikazu MORITA***

Synopsis

Quay walls designed with high seismic coefficients have been installed in many ports in Japan. Though one of these high seismic resistance quay walls experienced the 1995 Hyogo-ken nanbu earthquake and survived the disaster, it is necessary to clarify whether these quay walls can survive future earthquakes. The performance of high seismic resistance quay walls subjected to various levels of earthquake shaking is summarized in this paper.

The authors conducted a series of two-dimensional effective stress analyses on two gravity type quay walls. One is the usual type, which was designed with a seismic coefficient of 0.15, and was severely damaged in the Kobe earthquake. The other is a high seismic resistance type designed with a seismic coefficient of 0.25. The effective stress model used in the analyses is based on a multiple shear mechanism model defined in strain space. The model parameters for the analyses were determined from various geotechnical investigations. The results of numerical analyses on the deformation of the usual type quay walls agree with measured deformation of damaged quay walls. Furthermore, the results of numerical analyses on the high seismic resistance quay wall shows small deformation and are consistent with measured deformation of the quay wall in Kobe Port. The numerical analyses also reveal the mechanism and the reason why the high seismic resistance quay wall in Kobe Port survived in the severe earthquake disaster.

In order to identify the effect of liquefaction and the dependence on the input acceleration level, a series of parametric studies were conducted. The results indicate that even in the most severe condition in Kobe Port during 1995 Hyogo-ken nanbu earthquake, the residual deformation of high seismic resistance quay wall will be less than 1.0 m if soil improvement against liquefaction is completed.

The paper concludes that the installation of high seismic resistance quay walls is effective for Japanese ports and soil improvement against liquefaction is necessary for those high seismic resistance quay walls.

Key Words : Earthquake, Earthquake resistant quay wall, Deformation, Effective stress analysis

* Research Engineer, Geotechnical Earthquake Engineering Laboratory, Structural Division

** Chief of Geotechnical Earthquake Engineering Laboratory, Structural Division

*** Research Engineer, Structural Dynamics Laboratory, Structural Division

Port and Harbour Research Institute, 3-1-1 Nagase, Yokosuka 239-0826, Japan.

Tel: 0468-44-5028/Fax: 0468-44-0839, E-mail: ichii@ipc.phri.go.jp

耐震強化岸壁の耐震性能に関する有効応力解析

一井 康二 *・井合 進 **・森田 年一 ***

要 旨

兵庫県南部地震以後、震災時に備える防災拠点の中核的施設として耐震強化岸壁が日本各地に建設されている。こういった耐震性強化岸壁の有効性については兵庫県南部地震時に摩耶埠頭の耐震強化岸壁が無被災であった事例が知られているが、その無被災のメカニズムについては明らかにされていない。したがって、今後想定される地震に対しての耐震強化岸壁の耐震性能がどの程度のレベルにあるかも検討されていない。そこで、一般の耐震強化岸壁の耐震性能を検証することを目的として有効応力解析を行った。今回の研究では、神戸港のケーソン式岸壁や防波堤などの解析により適用性の確認された解析手法を用いて解析を実施した。

本研究で用いている有効応力モデルは、多重せん断機構に基づくものであり、阪神大震災における種々の建造物の被災の解析を通じてその適用性が確認されている。本研究では兵庫県南部地震時に無被災であった摩耶埠頭岸壁の無被災のメカニズムを解明した後、他の一般的な耐震強化岸壁の耐震性能について検討した。

有効応力解析の結果、摩耶埠頭岸壁の変位量は岸壁法線の方向性・ケーソン背後に埋め殺しされたセルの存在により小さく抑えられていたことがわかった。生じた変位量は主として置換砂部及び後背部の液状化によるものであり、液状化対策が施されていれば変形は全く生じなかったと思われる。一般の耐震強化岸壁についての検討では、液状化対策が施されていれば兵庫県南部地震における最もシビアな地震荷重条件の下でも変位量は1m以下に抑制できるとの見通しが得られた。

キーワード：地震、耐震強化岸壁、変形、有効応力解析

* 構造部 地盤震動研究室
** 構造部 地盤震動研究室長
*** 構造部 構造振動研究室

CONTENTS

Synopsis	79
1. Introduction	83
2. Outline of high seismic resistance quay wall in Kobe Port	83
3. Outline of the effective stress analysis method	88
3.1 Constitutive Equations	88
3.2 Finite element modeling	90
3.3 Model Parameters	91
3.4 Input Accelerations	96
4. Performance of high seismic resistance quay wall	98
4.1 Effect of the direction of the quay walls	98
4.2 The effect of the existence of the old steel cellular structure	104
4.3 The effect of ground liquefaction	105
5. High seismic resistant design of quay walls	106
5.1 Seismic performance relative to designed seismic coefficient	106
5.2 Level of improved liquefaction resistance	110
6. Conclusion	111
References	112

1. Introduction

On January 17, 1995, one of the most disastrous earthquakes called the 1995 Hyogoken-nanbu earthquake of JMA Magnitude 7.2, hit the Hanshin area of Japan. Kobe Port was shaken with a strong motion having peak ground acceleration of 0.54g and 0.45g in the horizontal and vertical directions respectively ¹⁾. Most of the quay walls in Kobe Port are of a rigid block type made of concrete caissons and were severely damaged by the earthquake. Quay walls moved about 5 m maximum, about 3 m on average, toward the sea. The walls also settled about 1 to 2 m and tilted about 4 degrees toward the sea. The mechanism of this large deformation was identified using effective stress analyses ²⁾ and shaking table tests ³⁾.

One quay wall at Maya Wharf was designed with a high seismic coefficient ($K_h=0.25$) and available for emergency use just after the earthquake disaster. Although the usual type quay walls were severely damaged, this high seismic resistance quay wall survived and was available for emergency use. This success of a high seismic resistance quay wall encouraged the construction of seismic resistance type quay walls in Japanese ports.

The mechanism of survival of the quay wall designed with high seismic resistance has not been identified. It is necessary to identify why this high seismic resistance quay wall survived and whether or not the same type of quay wall can survive in other earthquakes. In this paper, two-dimensional effective stress analyses are conducted to identify the deformation mechanism and determine why the high seismic resistance quay wall did not suffer severe deformation and damage.

2. Outline of high seismic resistance quay wall in Kobe Port

The location of the high seismic resistance quay wall at Maya Wharf is shown in **Figure 1**. It is located in the northern part of Kobe Port and the quay walls were constructed as steel cellular type quay walls in 1967. After construction of the original cellular type quay wall, three berths in Maya No.1 Wharf were improved as high seismic resistance quay walls with seismic coefficients of $K_h=0.25$. The northern berth of -10 m depth was improved as a pier type quay wall and the other two berths of -10 m depth and -12 m depth were improved as caisson type quay walls. The cross section of the high seismic resistance design quay wall of -10 m depth is shown in **Figure 2**. The old cellular structure still remains behind the caisson and backfill rock was placed between the caisson and the steel cellular structure. The foundation of the old cellular structure was improved with filled sand and the foundation of the caisson was improved with a gravel mound. Though most of the caisson type quay walls in Kobe Port are constructed on the deep clay layer improved with soil replacement, quay walls in Maya Wharf have a shallow clay layer to be improved.

The deformation of the quay walls after the earthquake shaking is shown in **Figure 3**. The concrete caisson is slightly inclined and moved about 1 to 2 m toward sea. The investigated deformation at the top of the caisson is summarized in **Figure 4**. Though horizontal displacement of 1 to 2 m toward the sea and settlement of tens of centimeters occurred, irregularity of displacement was not significant and the quay walls could be used immediately following the earthquake, as shown in **Photo 1**. Since the deformation of the quay walls was very limited and no irregular deformation was observed, it can be concluded that the quay walls didn't suffer significant damage.

Whereas the high seismic resistance quay walls did not suffer significant damage, usual type quay walls in Kobe Port were severely damaged. The displacements of quay walls at Port Island and Rokko Island are shown on **Figure 5**. Quay walls moved 5 m in maximum and about 3 m on average ¹⁾. The mechanism explains the differences in seismic performance has not been identified and there are several factors which affect the seismic performance of the high seismic resistance quay walls. For instance, the horizontal earthquake motion has a predominantly north-south direction as shown in **Figure 6** ⁴⁾ and the damage of quay walls with east-west face lines is more severe than that of the quay walls with north-south face lines as shown in **Figure 5**. Since the high seismic resistance quay walls in Maya Wharf have a north-south face line as shown in **Figure 1**, it is thought that the orientation of the face line

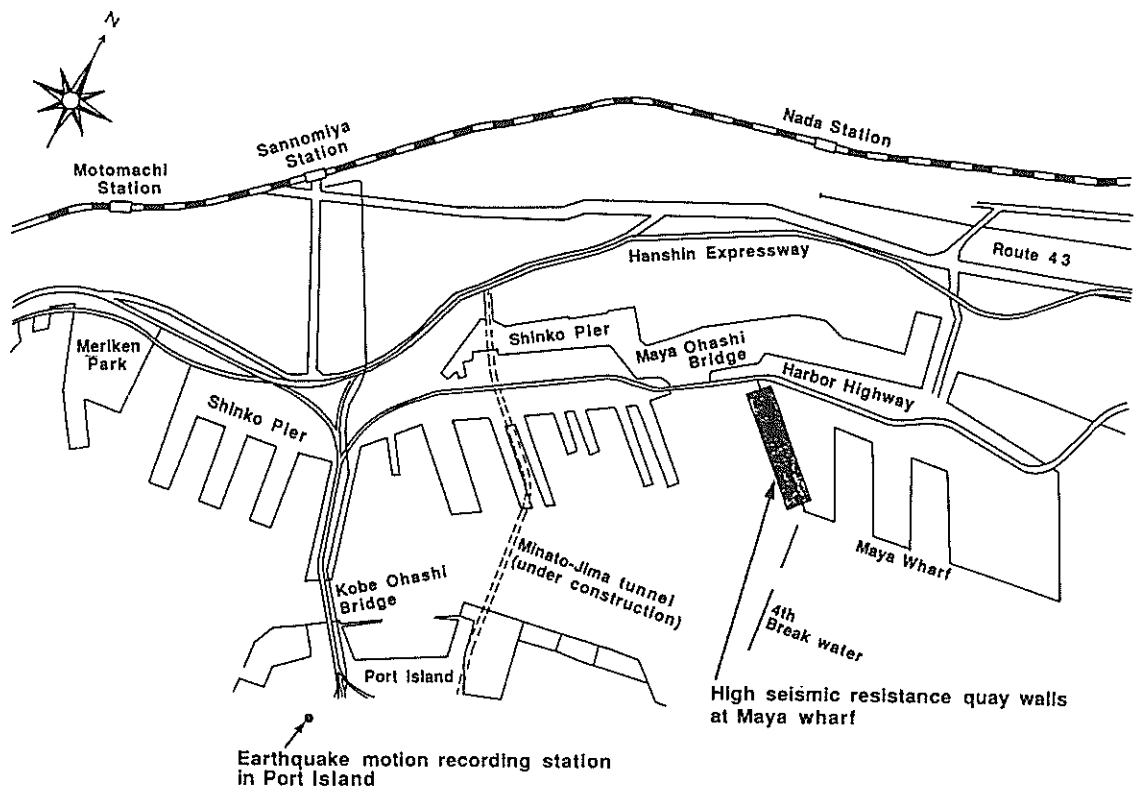
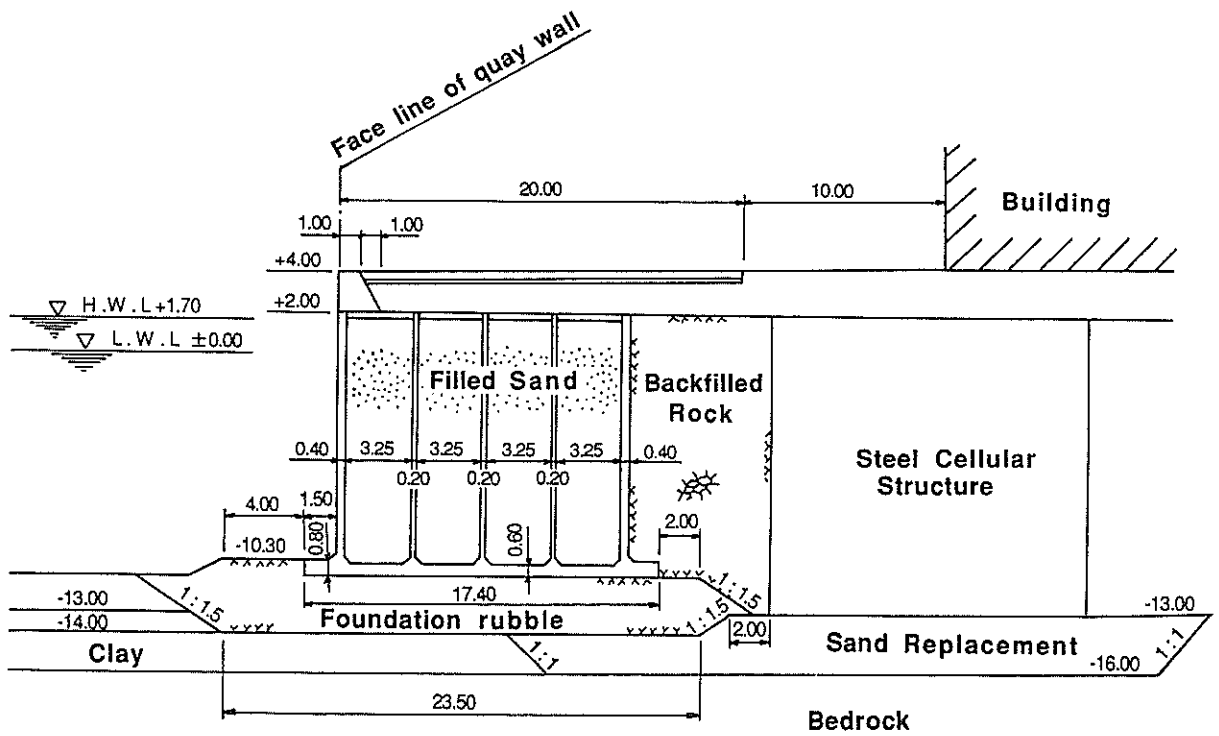


Figure 1 Location of high seismic resistance quay walls at Maya Wharf in Kobe Port



Units: m

Figure 2 Cross section of high seismic resistance quay wall with 10 m depth

parallel to the predominant horizontal direction of earthquake shaking is one of the reasons why these quay walls survived.

The possible factors which may have resulted in a lower deformation of quay walls are summarized as follows.

- (1) High seismic coefficient ($K_h=0.25$).
- (2) Existence of old steel cellular structure behind caisson.
- (3) Absence of weak foundation as liquefiable sand replacement under the caisson.
- (4) Face line of quay walls parallel to the predominant direction of earthquake shaking.

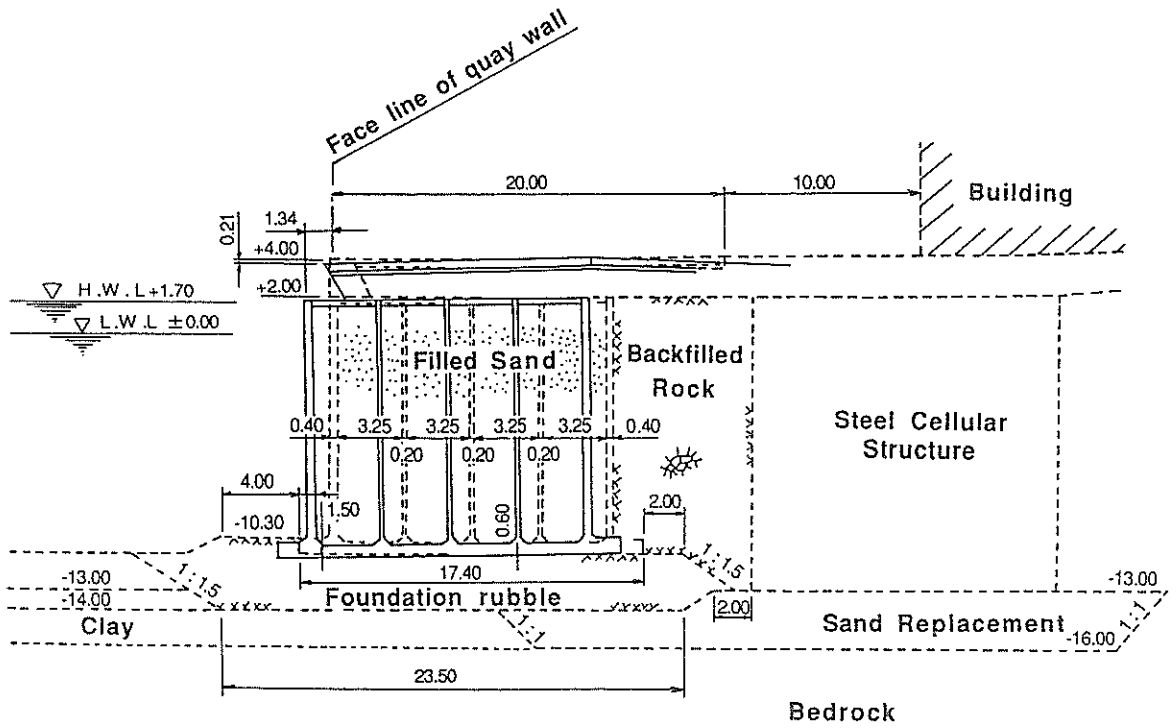
Therefore, why the high seismic designed quay walls survived in the earthquake is one of the most important issues to be discussed.



Photo 1 High seismic designed quay walls just after the earthquake



Photo 2 Deformation and settlement between caisson and cellular structure



Units: m

Figure 3 Deformation of high seismic resistance quay wall after the earthquake

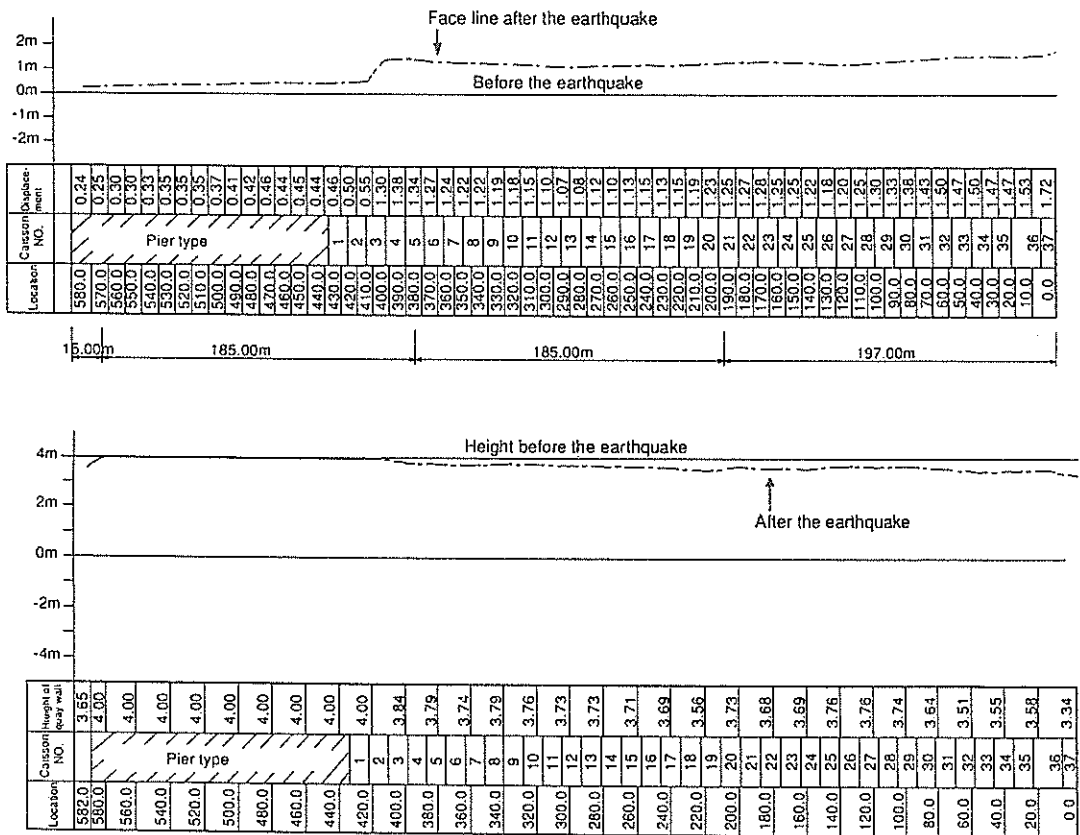


Figure 4 Investigated deformation of high seismic resistance quay walls in Maya Wharf

Performance of the Quay Walls with High Seismic Resistance

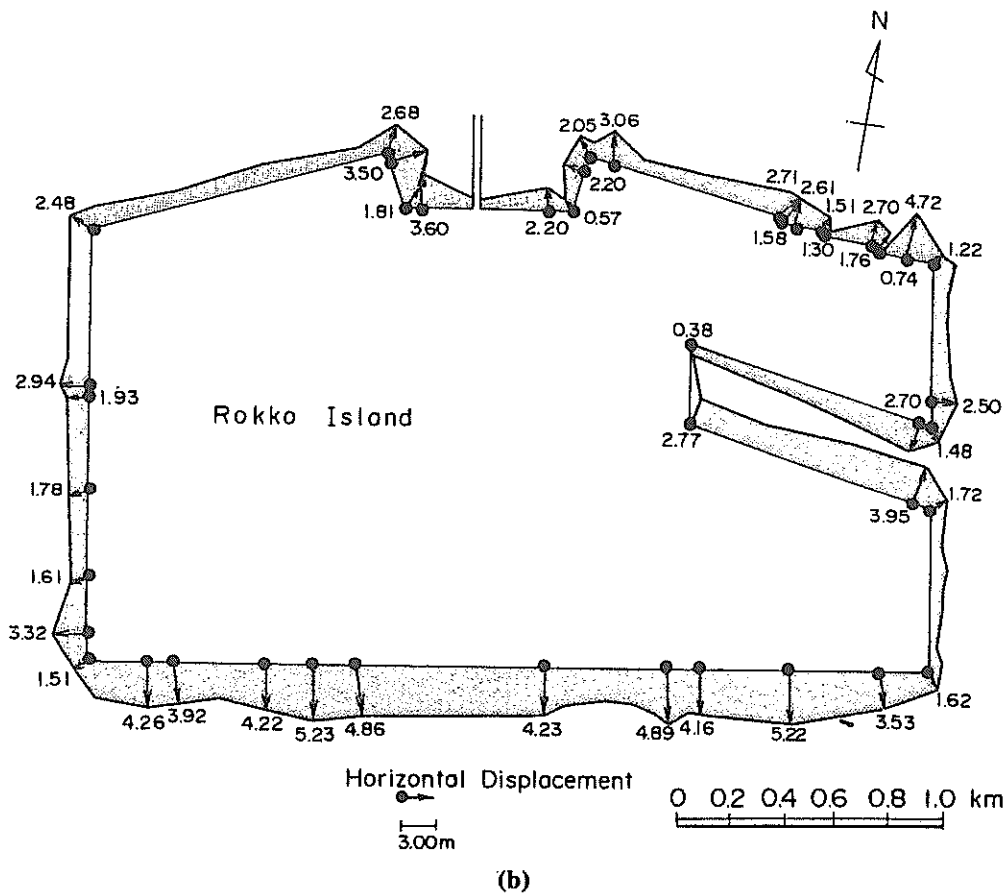
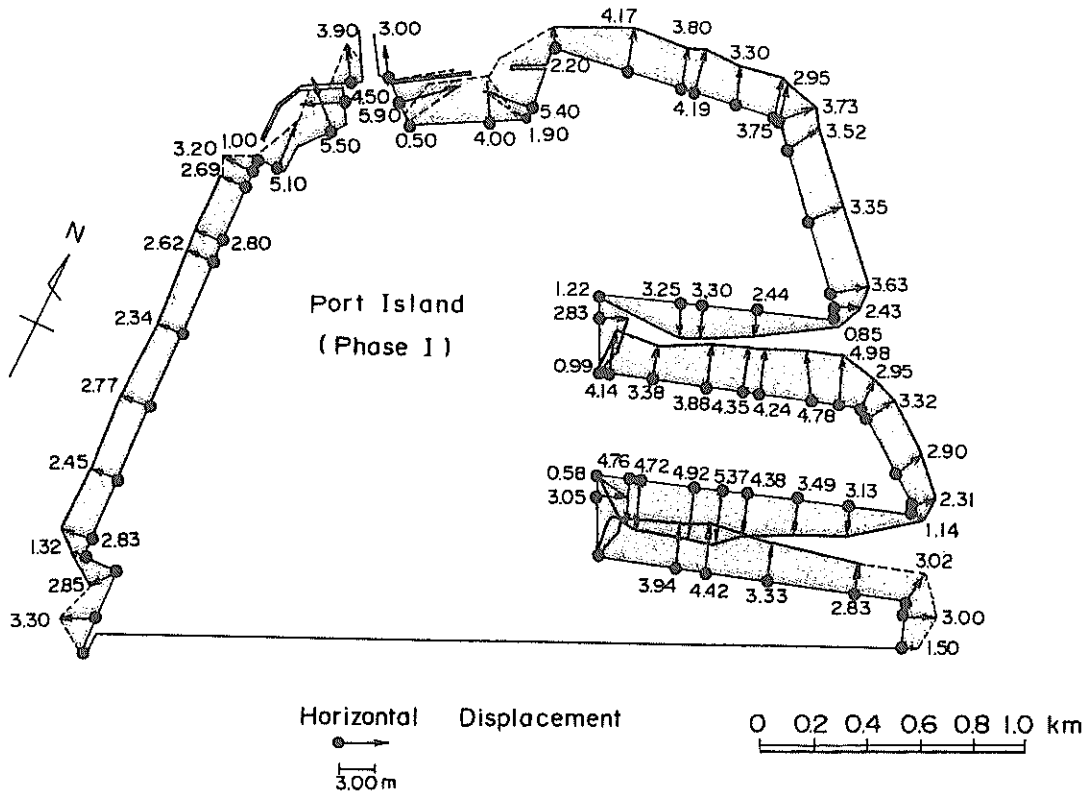
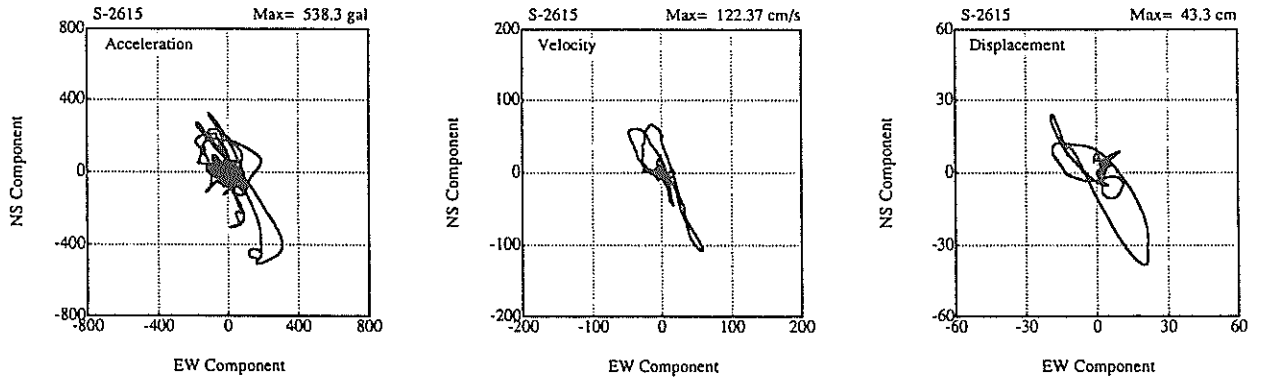


Figure 5 Displacement of quay walls at Port Island and Rokko Island



* Loci of acceleration, velocity, displacement calculated with fixed filter.

Figure 6 Orbit of acceleration, velocity, displacement of earthquake motion in Kobe Port

3. Outline of the effective stress analysis method

3.1 Constitutive Equations

The constitutive model used in this study is a strain space plasticity type and consists of a multiple shear mechanism in the plane strain condition⁵⁾. With the effective stress and strain vectors written by

$$\{\sigma'\}^T = \{\sigma'_x, \sigma'_y, \tau'_{xy}\} \quad (1)$$

$$\{\varepsilon\}^T = \{\varepsilon_x, \varepsilon_y, \gamma_{xy}\} \quad (2)$$

The basic form of the constitutive relation is given by

$$\{d\sigma'\} = [D](\{d\varepsilon\} - \{d\varepsilon_p\}) \quad (3)$$

in which

$$[D] = K \{n^{(0)}\} \{n^{(0)}\}^T + \sum_{i=1}^I R_{L/U}^{(i)} \{n^{(i)}\} \{n^{(i)}\}^T \quad (4)$$

In this relation, the term $\{d\varepsilon_p\}$ in Eq.(3) represents the additional strain incremental vector to take the dilatancy into account and is given from the volumetric strain increment due to the dilatancy as

$$\{d\varepsilon_p\}^T = \{d\varepsilon_p / 2, d\varepsilon_p / 2, 0\} \quad (5)$$

The first term in Eq.(4) represents the volumetric mechanism with rebound modulus K and the direction vector is given by

$$\{n^{(0)}\}^T = \{1, 1, 0\} \quad (6)$$

The second term in Eq.(4) represents the multiple shear mechanism. Each mechanism $i = 1, 2, \dots, I$ represents a virtual simple shear mechanism, with each simple shear plane oriented at an angle $\theta_i / 2 + \pi / 4$ relative to the x axis.

The tangential shear modulus $R_{L/U}^{(i)}$ represents the hyperbolic stress strain relationship with hysteresis characteristics. The direction vectors for the multiple shear mechanism in Eq.(4) are given by

$$\{n^{(i)}\}^T = \{\cos \theta_i, -\cos \theta_i, \sin \theta_i\} \quad (\text{for } i=1, 2, \dots, I) \quad (7)$$

in which

$$\theta_i = (i-1)\Delta\theta \quad (\text{for } i=1, 2, \dots, I) \quad (8)$$

$$\Delta\theta = \pi / I \quad (9)$$

A schematic figure for the multiple simple shear mechanism is shown in Figure 7. Pairs of circles indicate mobilized virtual shear strain in positive and negative modes of compression shear (solid lines with darker hatching) and simple shear (broken lines with lighter hatching).

The loading and unloading for the shear mechanism are separately defined for each virtual simple shear mechanism by the sign of $\{n^{(i)}\}^T \{d\varepsilon\}$. The multiple shear mechanism takes into account the effect of rotation of the principal stress axis directions, the effect of which is known to play an important role in the cyclic behavior of anisotropically consolidated sand ⁶. Ten parameters are needed for the present model: two of which characterize elastic properties of soil, another two specify plastic shear behavior, and the rest characterize dilatancy, as shown in Table 1.

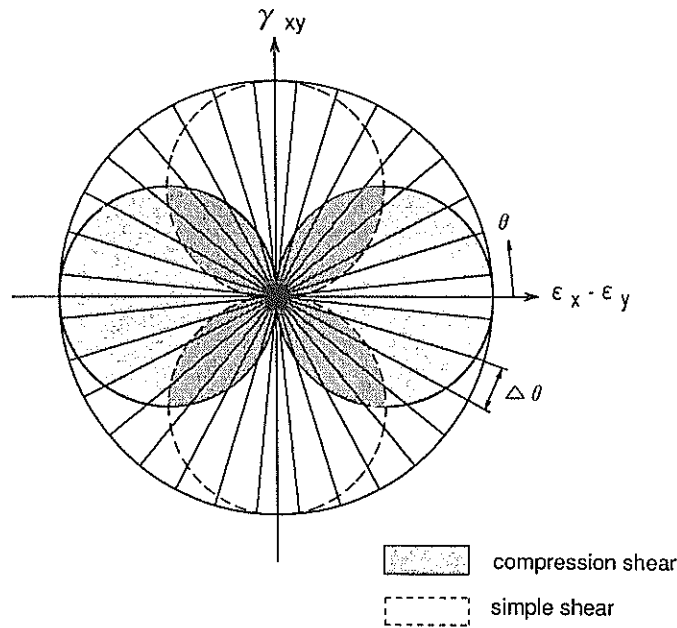


Figure 7 Schematic figure for the multiple simple shear mechanism

Table 1 Parameters of the present model

Parameters	Type of Mechanism	Kind of the parameters
K_a	Elastic volumetric	Rebound modulus
G_{ma}	Elastic shear	Shear modulus
ϕ_f	Plastic shear	Shear resistance angle
ϕ_p	Plastic dilatancy	Phase transformation angle
H_m	Plastic shear	Hysteretic damping factor at large shear strain level
p_1	Plastic dilatancy	Initial phase of dilatancy
p_2	Plastic dilatancy	Final phase of dilatancy
w_1	Plastic dilatancy	Overall dilatancy
S_1	Plastic dilatancy	Ultimate limit of dilatancy
c_1	Plastic dilatancy	Threshold limit of dilatancy

3.2 Finite element modeling

The finite element mesh shown in Figure 8 was used for the analysis under plane strain conditions. A total of 586 nodal points and 840 elements including pore water elements were used. Five types of elements were used in the analysis: linear elements for the caisson, nonlinear elements for sand and clay, beam elements for the steel cellular structure, liquid elements for water, and joint elements for the boundaries between soil and structure. The sea water was modeled as incompressible fluid and was formulated as an added mass matrix based on the equilibrium and continuity of fluid at the solid-fluid interface ⁷⁾. The computer program code named FLIP (Finite element analysis of Liquefaction Program) was used in this analyses ⁵⁾.

Modeling of the steel cellular structure is one of the most difficult points to be discussed. In this paper, we assume the cellular structure possesses enough strength and rigidity to perform as a rigid block. As shown in Figure 9, the cellular structure consists of two vertical rigid beam elements with soil elements in between and two diagonal rigid beam for additional strength. Continuity of soil elements inside the cellular structure and beneath the cellular structure was kept in this modeling. Joint elements at the front and backside of the cellular structure can express slip or separation between the cellular structure and soil. The validity of modeling is examined in the comparison with analyzed cases with and without the cellular structure in the later chapter.

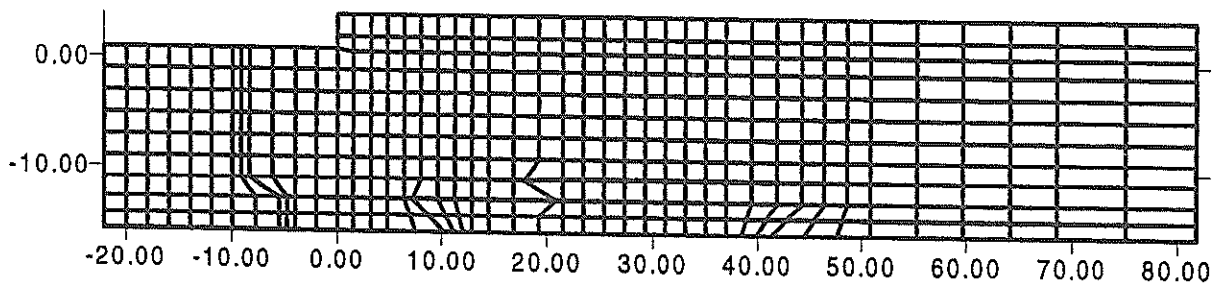


Figure 8 The mesh for finite element analysis

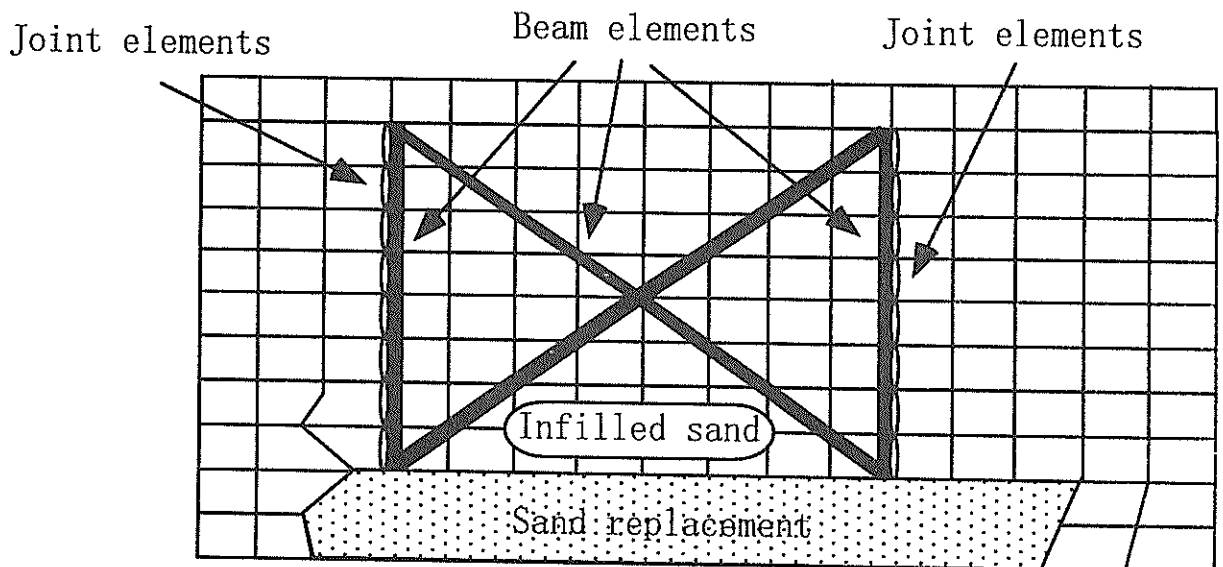


Figure 9 Schematic figure for the modeling of cellular structure

3.3 Model Parameters

The model parameters were estimated by referring to the geotechnical investigation results. Figures 10 and 11 show the locations and results of the geotechnical investigations at Maya Wharf, respectively. The parameters for backfilled sand and the sand replacement layer were estimated based on the SPT N values for the sand replacement layer at 17 m to 20 m depth. Since SPT N values in the sand replacement layer were scattered within wide range (5 to 40), both obtained the upper and lower extreme values were eliminated and an SPT N value between 10 to 20 was obtained. Considering the effect of overburden pressure, the equivalent SPT N value (corrected for 0.66kg/cm^2 overburden pressure) for the sand replacement layer is 5 to 10. Thus medium value of 8 was used for parameter calibration and the simplified method for parameter determination was applied⁸⁾.

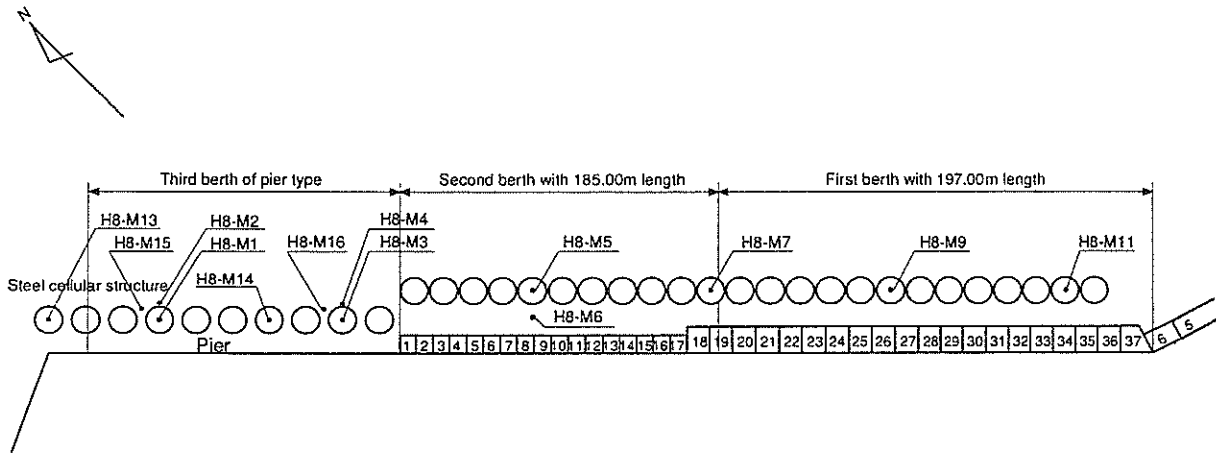


Figure 10 Locations of the geotechnical investigations at the Maya Wharf

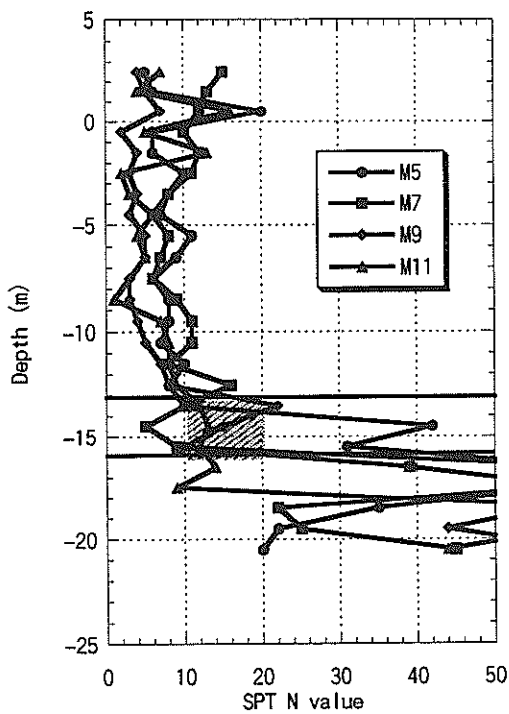


Figure 11 SPT N values investigated at the Maya Wharf No.1 and No.2 berth (caisson type berths)

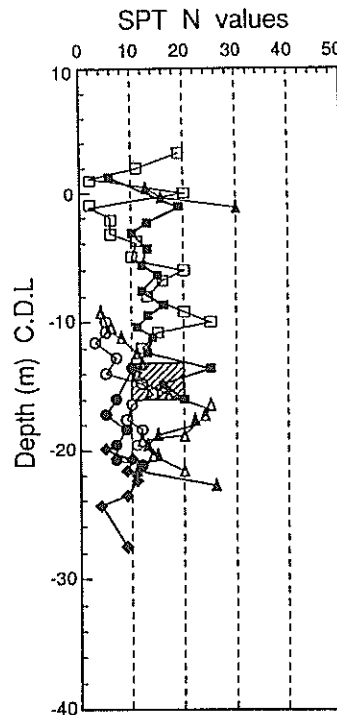


Figure 12 SPT N values in Port Island

The dilatancy parameters for sand were determined based on geotechnical investigation results including in-situ freezing sampling at Port Island, which was reclaimed with almost the same sand as that used at Maya Wharf. SPT N values of backfilled sand and replacement sand in Port Island are shown in Figure 12. For the same depth as the sand replacement at Maya Wharf (K.P.-13m to -16m), SPT N values from Port Island are scattered between 10 and 20, which indicates almost the same equivalent SPT N value as the sand replacement layer at Maya Wharf. Therefore, the liquefaction resistance for the sand replacement layer at Maya Wharf is estimated using the large scale cyclic triaxial tests results from in-situ freezing sampling at Port Island.

An example of the large scale cyclic triaxial tests using in-situ freezing sampling at Port Island is shown in Figures 13 to 15⁹⁾. There is not much difference between the liquefaction resistance for backfilled sand and sand used replacement layer which is shown in Figure 16. With these test results, we conducted a numerical simulation of the triaxial test and calibrated the parameters using the trial and error method. An example of the numerical simulation results of the triaxial test is shown in Figures 17 to 19. The liquefaction resistance for sand replacement layer at Maya Wharf is summarized in Figure 20. Since there is no difference between the liquefaction resistance for backfilled sand and sand used for replacement as shown in Figure 20, we used the same liquefaction resistance parameter for both sands in the analyses of Maya Wharf. Since the characteristics of the clayey layer might be uniform in Kobe Port, the parameters calibrated for clayey layer of Rokko Island²⁾ was used in this analyses. The parameters for analyses are summarized in Table 2.

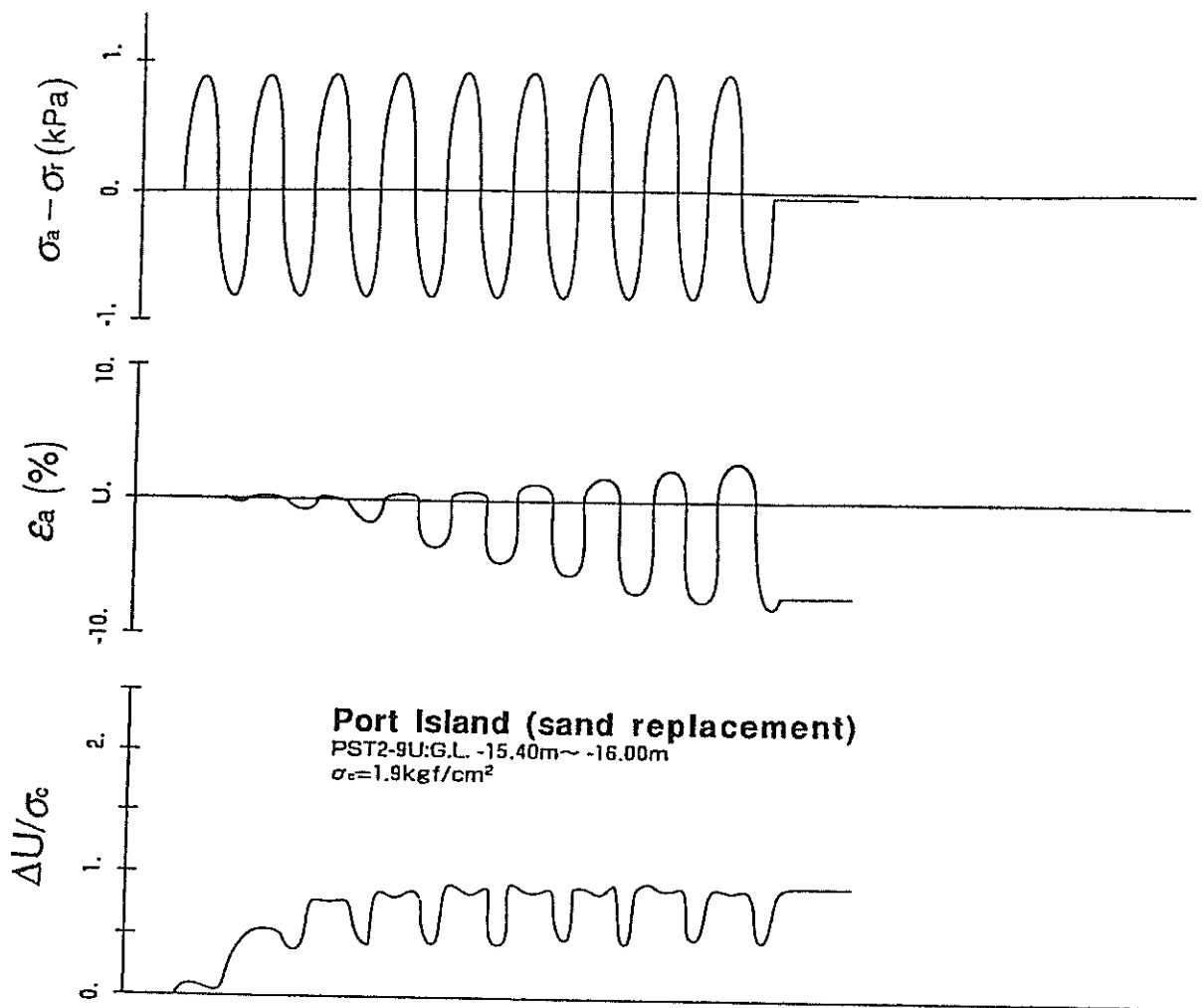


Figure 13 An example of stress, strain and pore water pressure time history in triaxial tests

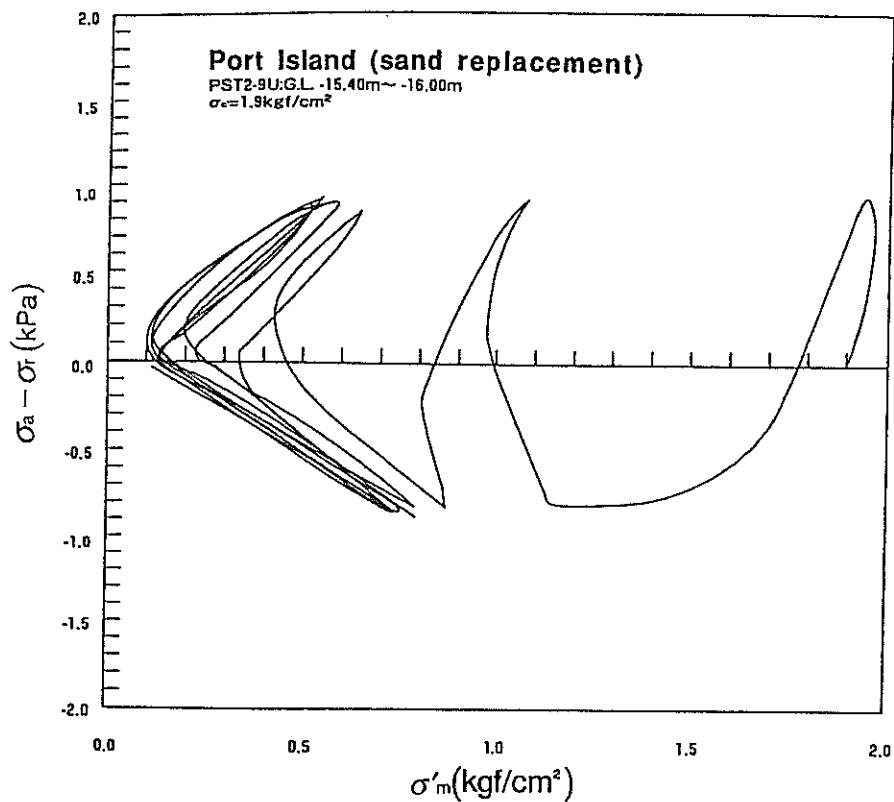


Figure 14 An example of stress path in triaxial tests

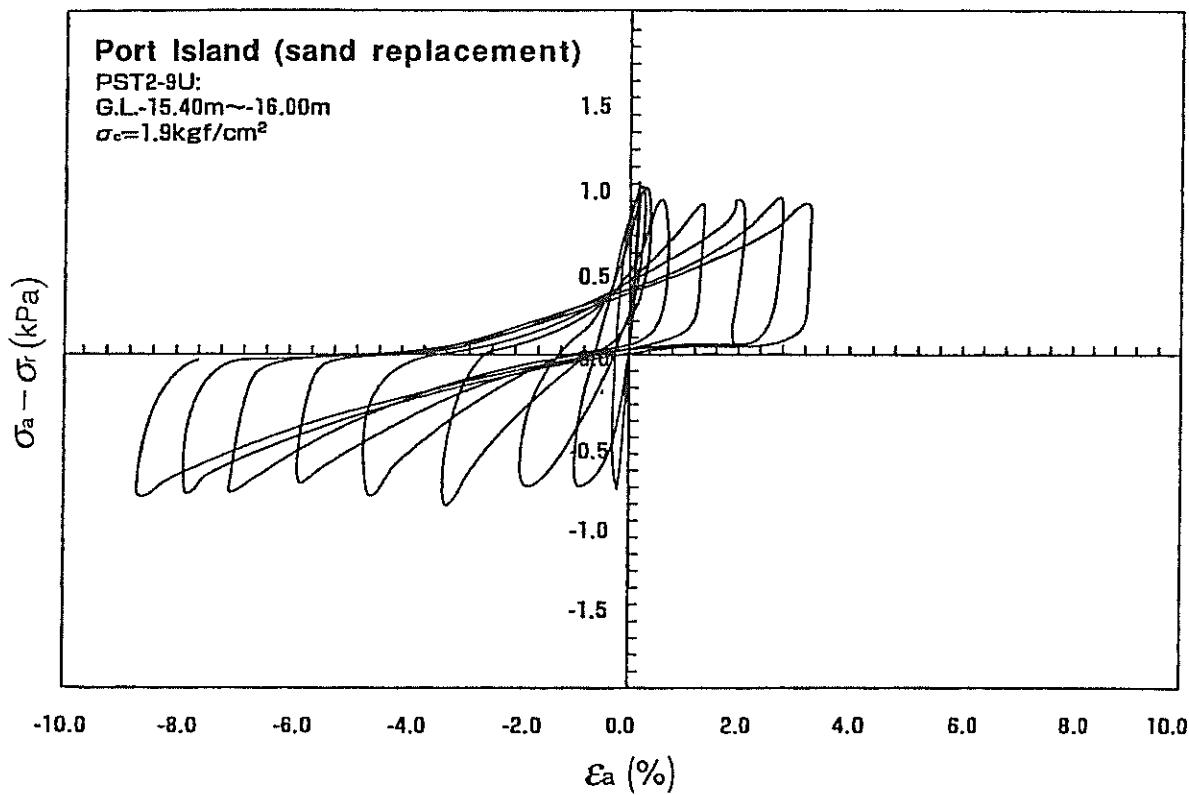


Figure 15 An example of stress-strain relation in triaxial tests

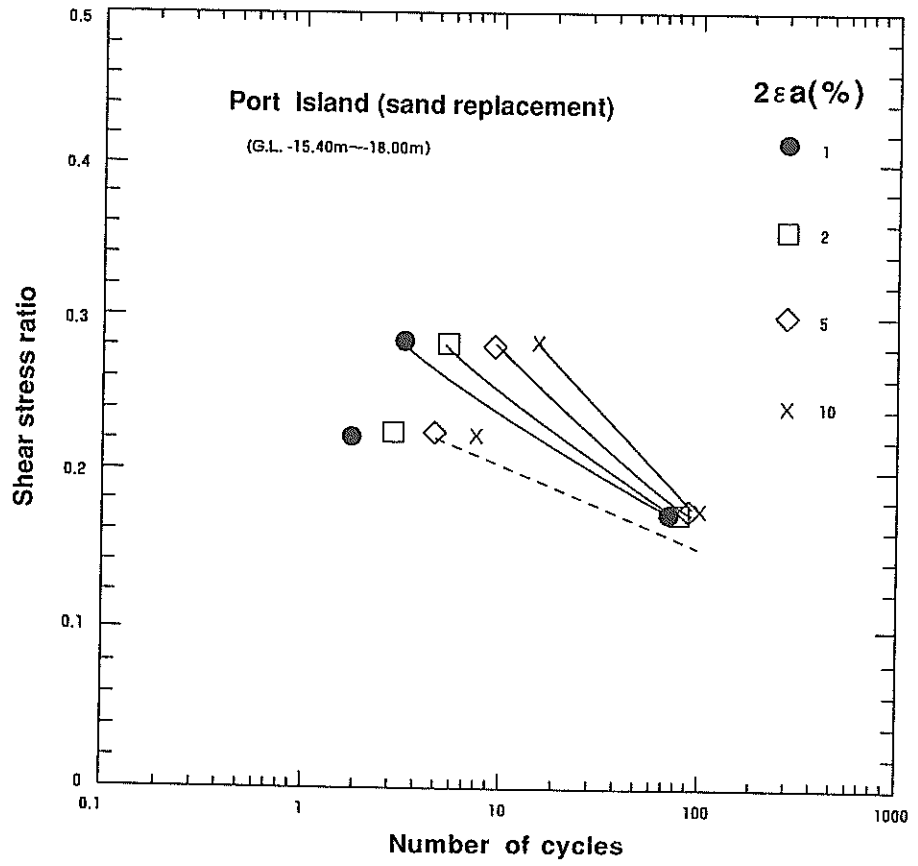


Figure 16 Liquefaction resistance for Port Island sand

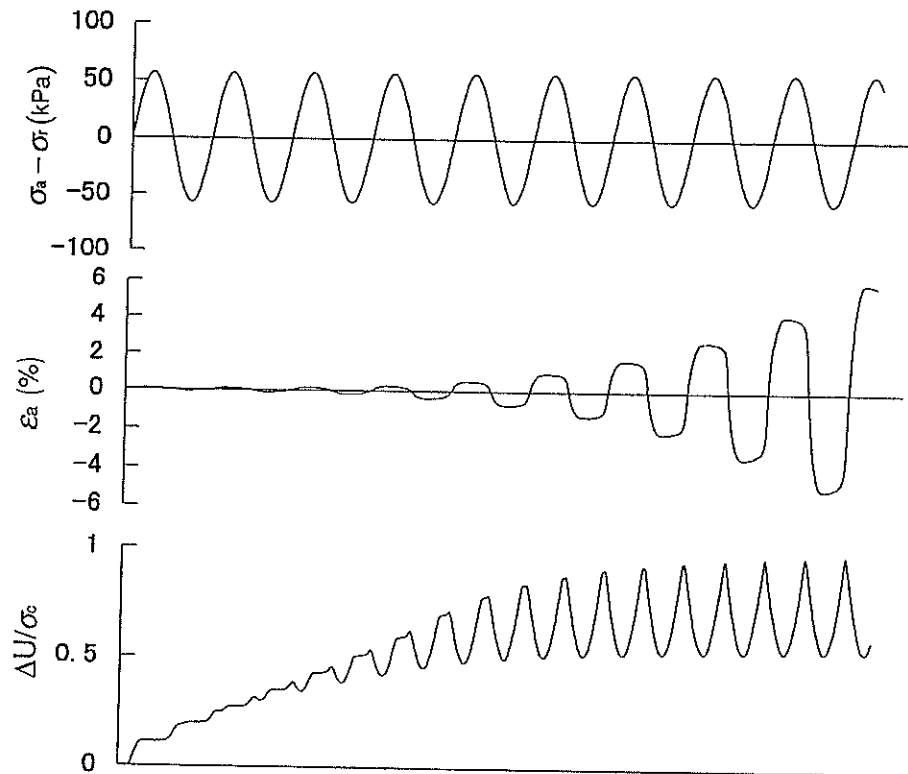


Figure 17 An example of computed stress, strain and pore water pressure time history

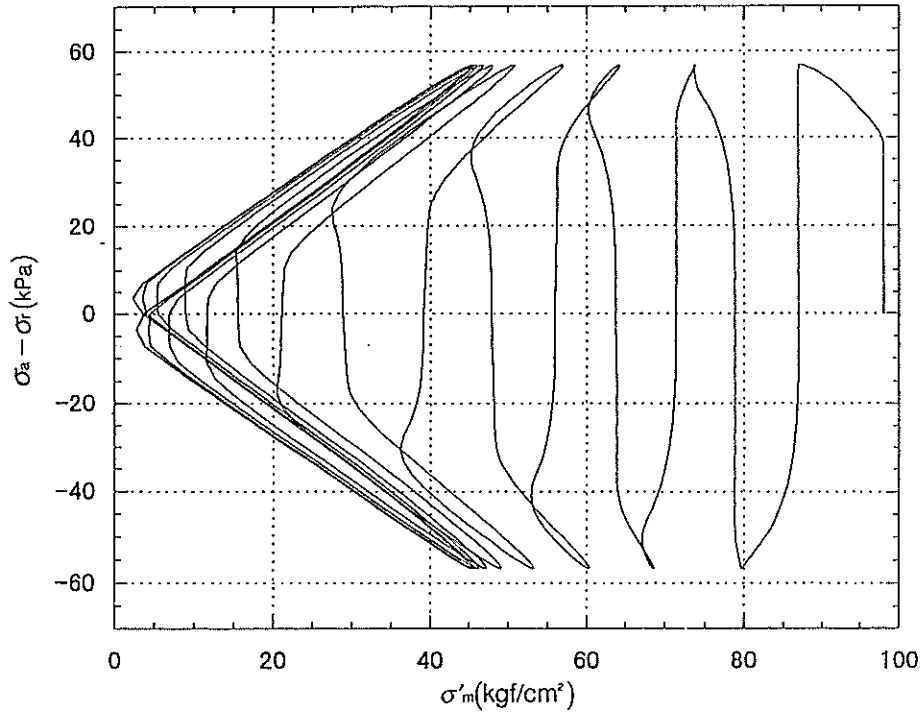


Figure 18 An example of computed stress path

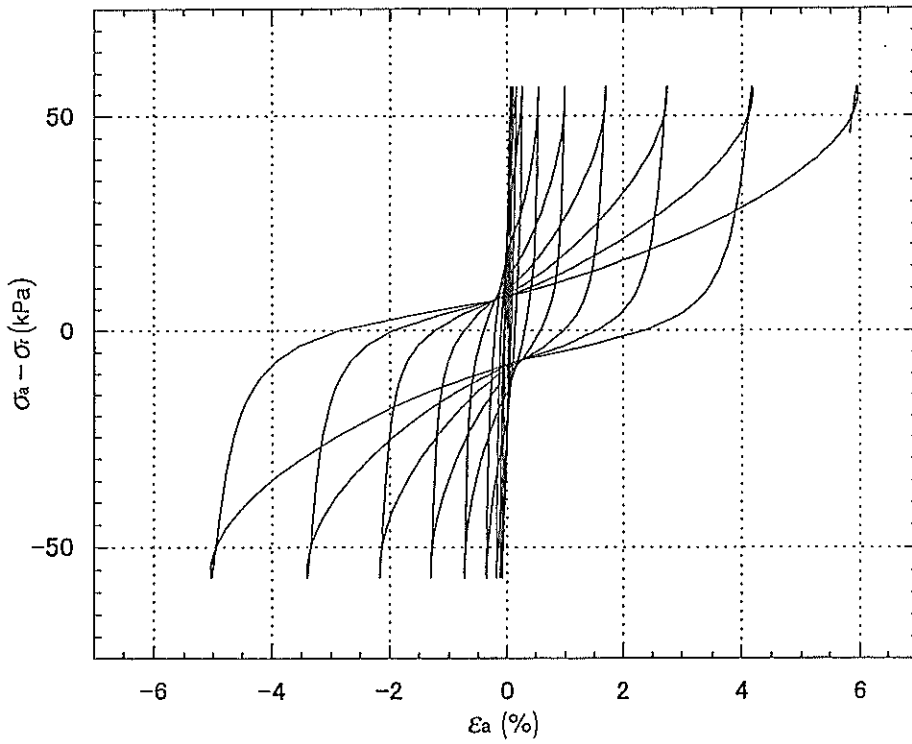


Figure 19 An example of computed stress-strain relation

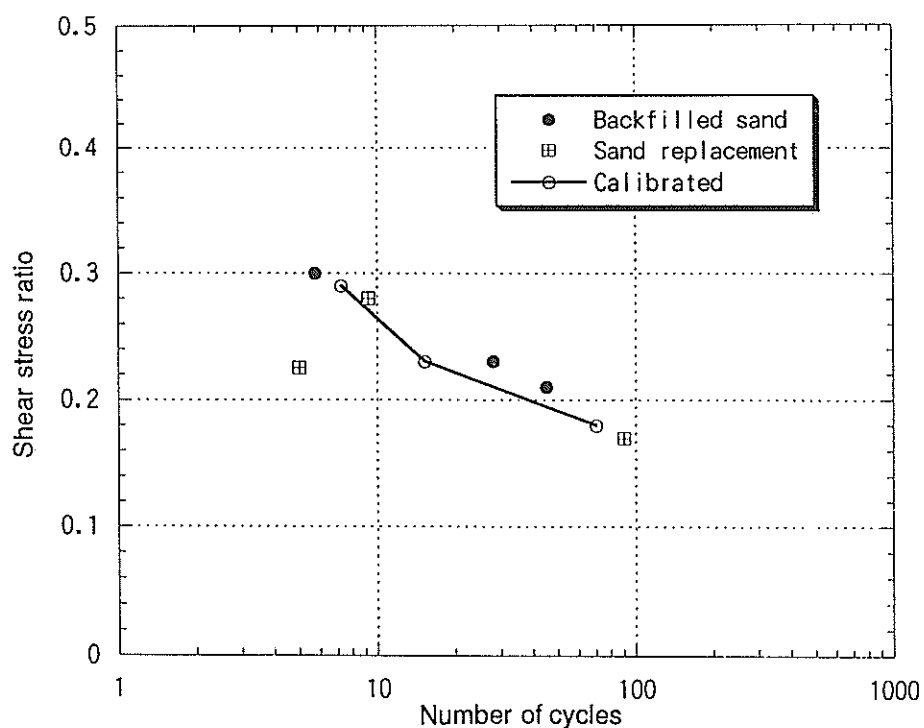


Figure 20 Computed liquefaction resistance for sand replacement layer at Maya Wharf

Table 2 Parameters used for the analyses

Layer No.	γ (tf/m ³)	G_a (kPa)	K_{ma} (kPa)	σ'_{ma} (kPa)	ϕ_f (deg.)	ϕ_p (deg.)	Parameters for dilatancy				
							S_1	w_l	p_1	p_2	c_1
Filled sand	2.00	67620	176000	98.0	39.4	28	0.005	6.5	0.5	1.0	2.10
Sand replacement	2.00	67620	176000	98.0	39.4	28	0.005	6.5	0.5	1.0	2.10
Filled rock	2.00	180000	469000	98.0	40.0						
Mound rock	2.00	180000	469000	98.0	40.0						
Clay layer	1.70	74970	195500	143.0	30.0						

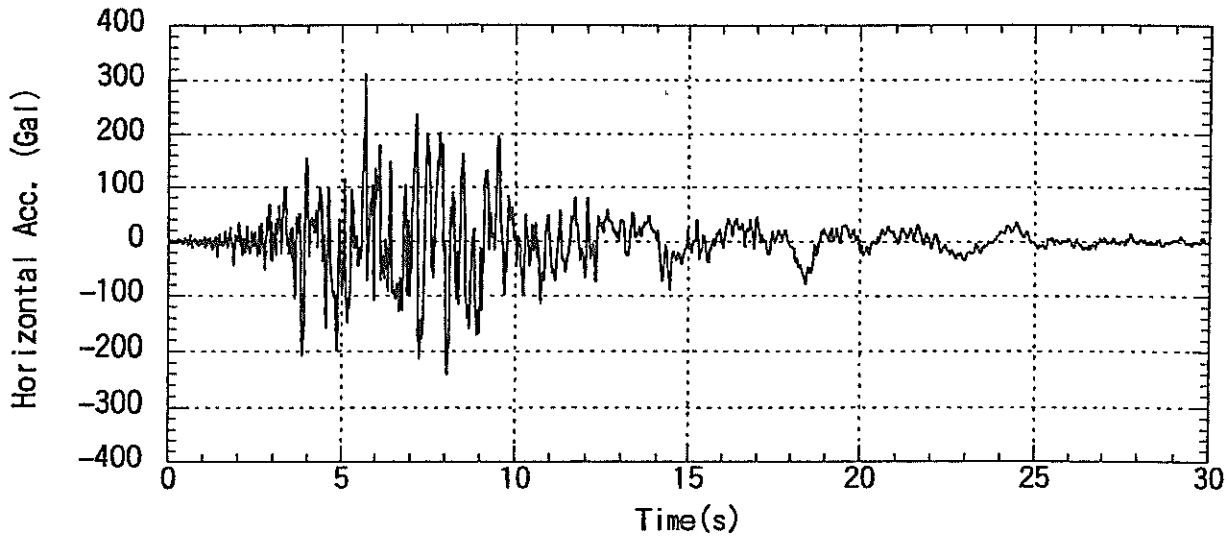
3.4 Input Accelerations

The earthquake motion was recorded by a vertical seismic array in Port Island at the ground surface and at depths of 16 m, 32 m and 83 m. The recording was successfully accomplished by Kobe City¹⁰⁾.

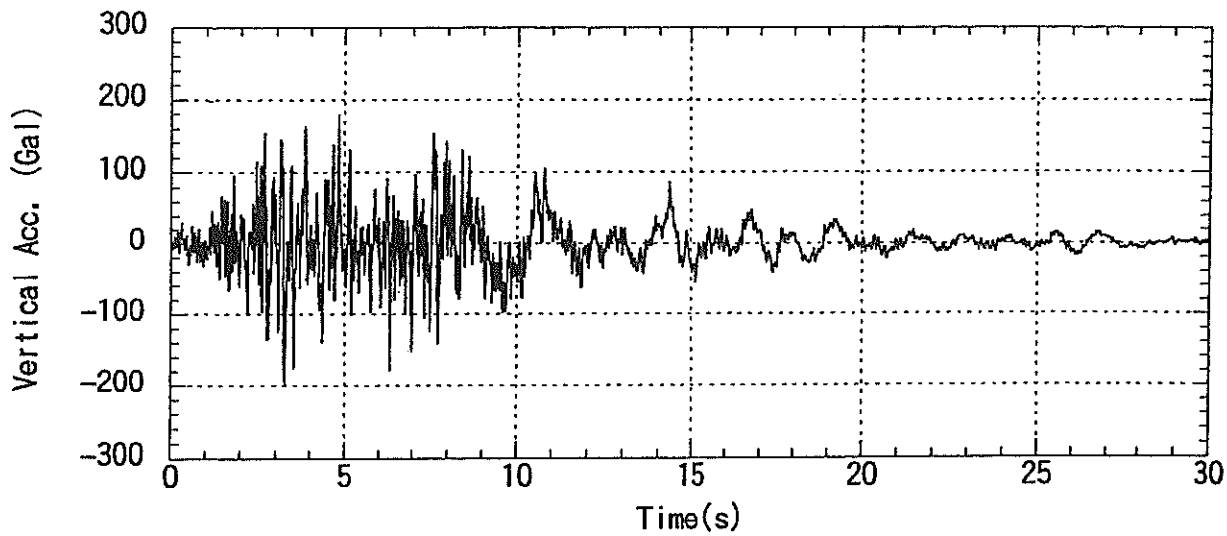
The vertical seismic array is located close to Maya Wharf, at a distance of about 3 km. The records at the depth of 32m shown in Figure 21 were used as the bedrock motion in the effective stress analysis. Since the analyses were conducted in two dimensions, the earthquake perpendicular to the face line of quay wall was used for the input motion. The maximum horizontal acceleration is 311 Gal in the horizontal direction, while the maximum vertical acceleration is 200 Gal.

Before the dynamic response analysis, a static analysis was performed to simulate the initial stress distributions to take the effect of gravity into account. The same constitutive model was used as in the earthquake response analysis, but the static analysis was performed under drained conditions. With these initial conditions and the

parameters mentioned earlier, an earthquake response analysis was performed on the high seismic resistance quay walls. To simplify the analysis, it was conducted under undrained conditions. The numerical time integration was made based on the Wilson- θ method ($\theta=1.4$) using the time interval of 0.01 seconds. Rayleigh damping ($\alpha=0$ and $\beta=0.002$) was used to ensure the stability of the numerical solution process.



(a) Horizontal component perpendicular to the face line of quay walls



(b) Vertical component

Figure 21 Input acceleration for the analyses recorded by Kobe City in Port Island at GL -32m

4. Performance of high seismic resistance quay wall

4.1 Effect of the direction of the quay walls

Using the aforementioned parameters, effective stress analyses were conducted. The final deformation and the excess pore water pressure ratio are shown in Figures 22 and 23 respectively. Liquefaction behind the cellular structure was observed and the ground surface settled about 20 to 30 cm in this area. The caisson moved toward the sea and tilted slightly. Settlement of the filled rock between the caisson and the cellular structure was observed. The magnified deformation pattern (magnification x4) shown in Figure 24 agrees with the observed settlements shown in Photo 2. Since no soil improvement was done at the seaside clayey layer, large shear strain of the soil elements was observed in this clayey layers and large deformation of this clayey layer occurred. Therefore, deformation can be reduced if soil improvement is conducted at the seaside clayey layer where large shear strains were observed.

Horizontal displacement at the top of the caisson was about 0.6 m toward the sea, which is fairly smaller than the observed deformation of 1.2 m. The major factor which may have reduced the deformation could be the absence of the effect of shaking parallel to the face line of the quay wall. Since the analysis was conducted in two dimensions, earthquake motion parallel to the face line of quay wall, which is the predominant direction of earthquake shaking, can not be considered. But liquefaction resistance of soils might be affected by this parallel shaking. Therefore, in this analysis, liquefaction resistance might be overestimated since we consider only one-directional shaking in the horizontal plane which is least likely cause liquefaction. In order to consider the effect of earthquake motion parallel to the face line, liquefaction resistance under multiple directional shear should be considered.

Some research exists on liquefaction resistance under multiple directional shear and the results are summarized in Figure 25¹¹⁾. In Figure 25, the horizontal axis shows the ratio of shear stress in two directions, τ_b/τ_a , and the vertical axis indicates the ratio of shear stress in two directional shear, τ_a , and one-directional shear τ_1 . Here, τ_a is the greater one in two directional shear and τ_1 is the one-directional shear component which would cause liquefaction equivalent to that caused by the combination of two-directional shear τ_a and τ_b . The triangle marker in Figure 25 shows the test results for saturated sand and circle shows the estimated value from the test results of dry sand. The dark hatched area in Figure 25 shows the area of calculated values using test results. Though the results are scattered, the research indicates that liquefaction resistance under two-directional shaking is 10 to 30% lower than that under one-directional shaking.

The analysis of Maya Wharf is more complicated than the situation represented by the analytical modeling. The motion parallel to the face line of the quay walls is greater than the perpendicular motion, which is used in the analysis. Therefore liquefaction resistance might be significantly lower than predicted, possibly more than 30% lower than predicted by the one-directional shaking analysis. A series of parametric analyses with liquefaction resistance reduced by 10 to 40% were conducted. Reduced liquefaction resistance and computed horizontal displacement under reduced liquefaction resistance are shown in Figures 26 and 27, respectively. The calculated displacement agrees with the observed displacement (indicated a dark hatch) when the analysis is performed using a 30 to 40% reduction in liquefaction resistance. The residual deformation and excess pore water pressure ratio under 30% reduced liquefaction resistance are shown in Figures 28 and 29 respectively. Though the magnitude of the deformation increased, the mode of deformation has no change. The excess pore water pressure ratio in both the sand replacement layer and the backfilled sand increased to about 0.8 or 0.9, and these sands were almost liquefied.

The acceleration and displacement time histories at the top of the caisson are shown in Figures 30 and 31 respectively. Though shaking with a period of 2 seconds exists in the horizontal acceleration time history, shaking with a period of 2 seconds is not observed in the vertical acceleration time history as shown in Figure 30. It can be considered that the horizontal response of 2 second period shaking is induced by the input horizontal acceleration which has a pulse of 2 seconds. Furthermore, though rocking shaking of a caisson is major in the analysis of usual caisson type quay walls¹²⁾, rocking shaking is minor in this analysis because of the absence of a deep sand

replacement layer under the caisson.

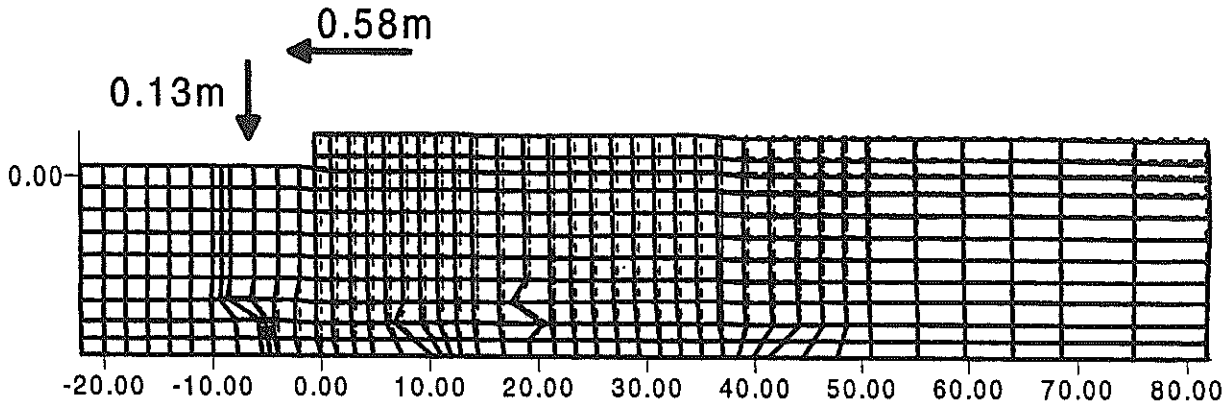


Figure 22 Computed deformation after the earthquake

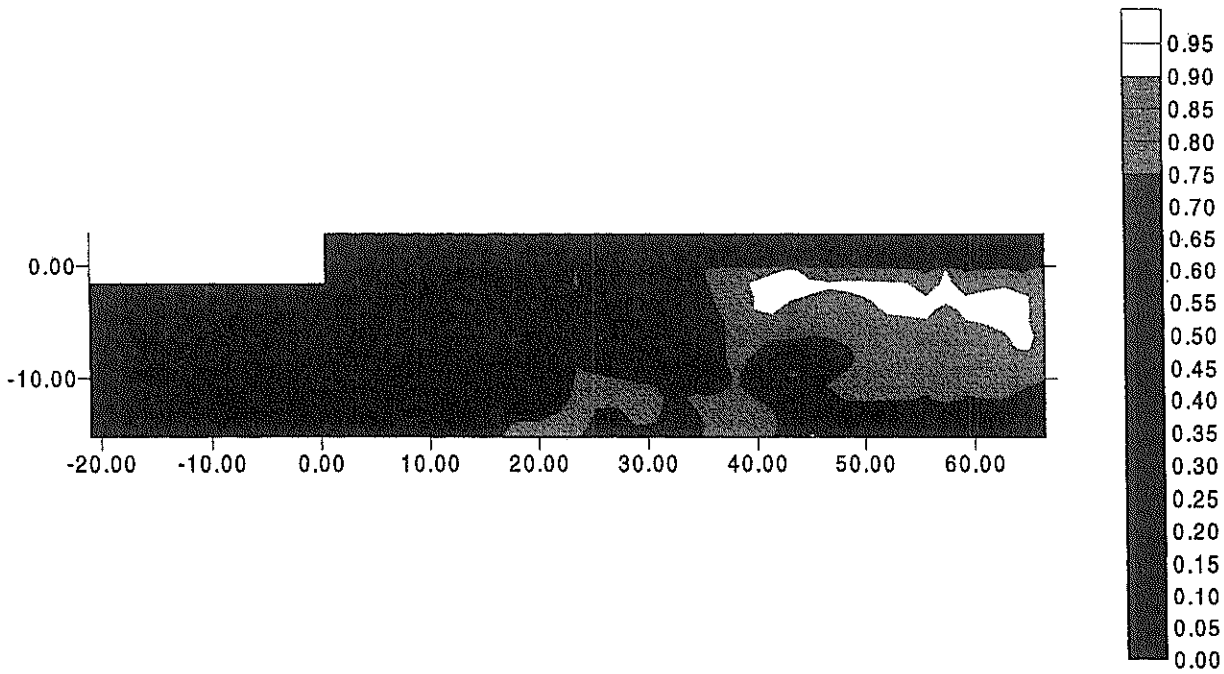


Figure 23 Computed excess pore water pressure ratio after the earthquake

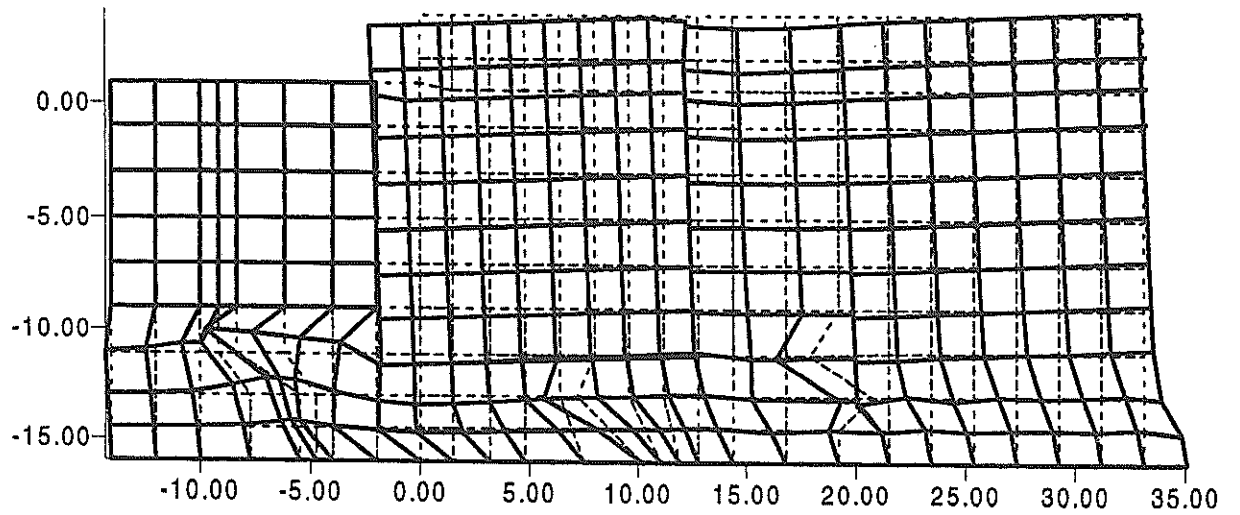


Figure 24 Deformation pattern around caisson in 4 times magnified scale

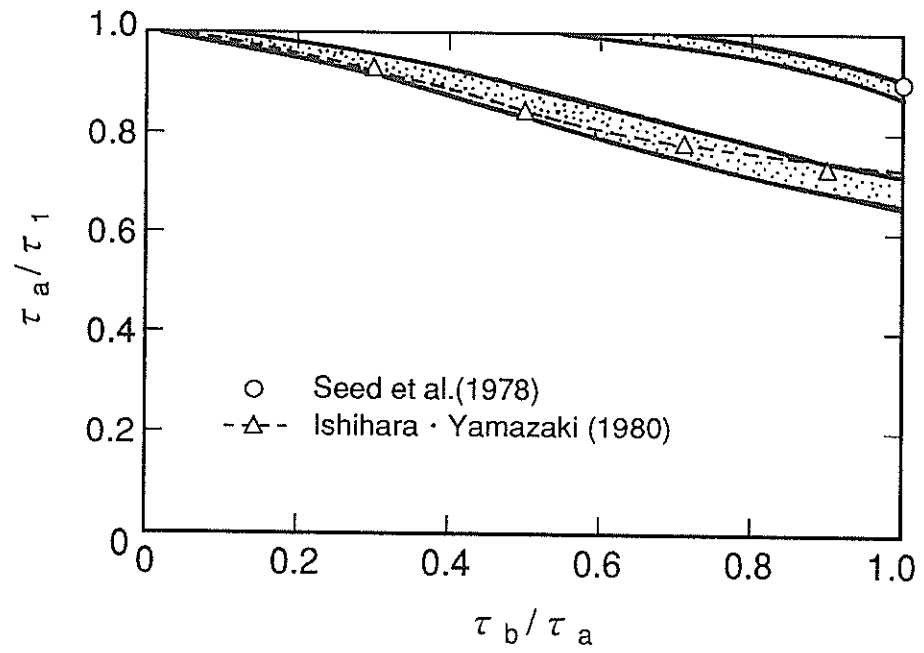


Figure 25 Reduction of liquefaction resistance under multiple shear (after Yoshimi, 1991)

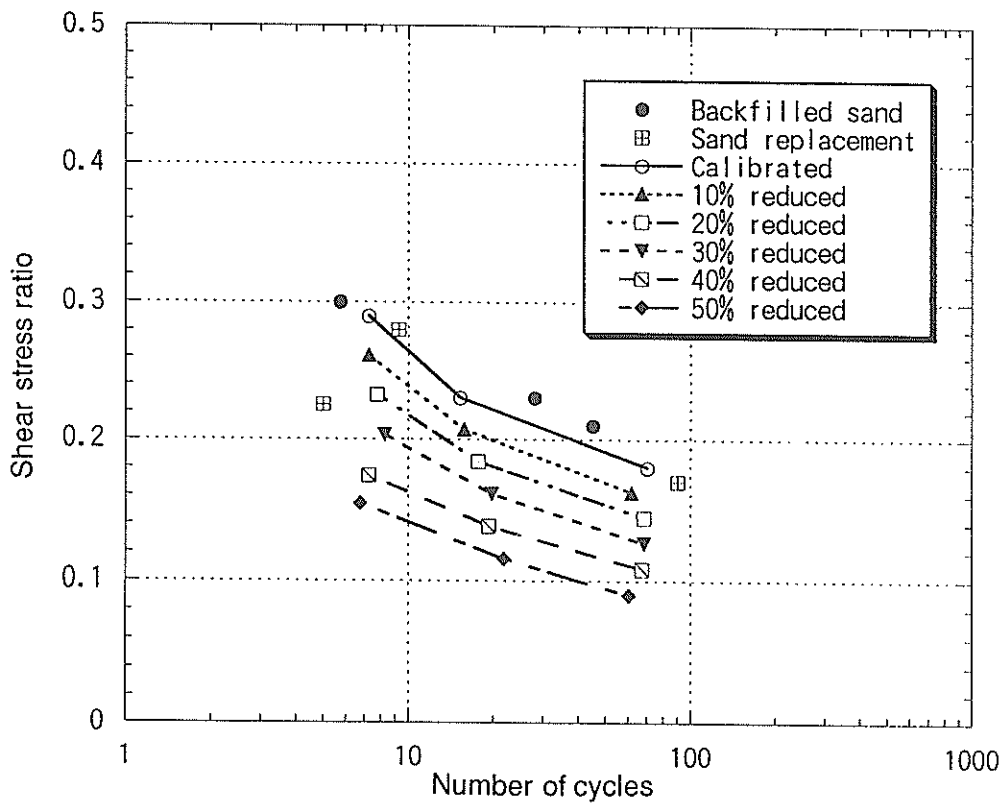


Figure 26 Reduced liquefaction resistance for parametric study

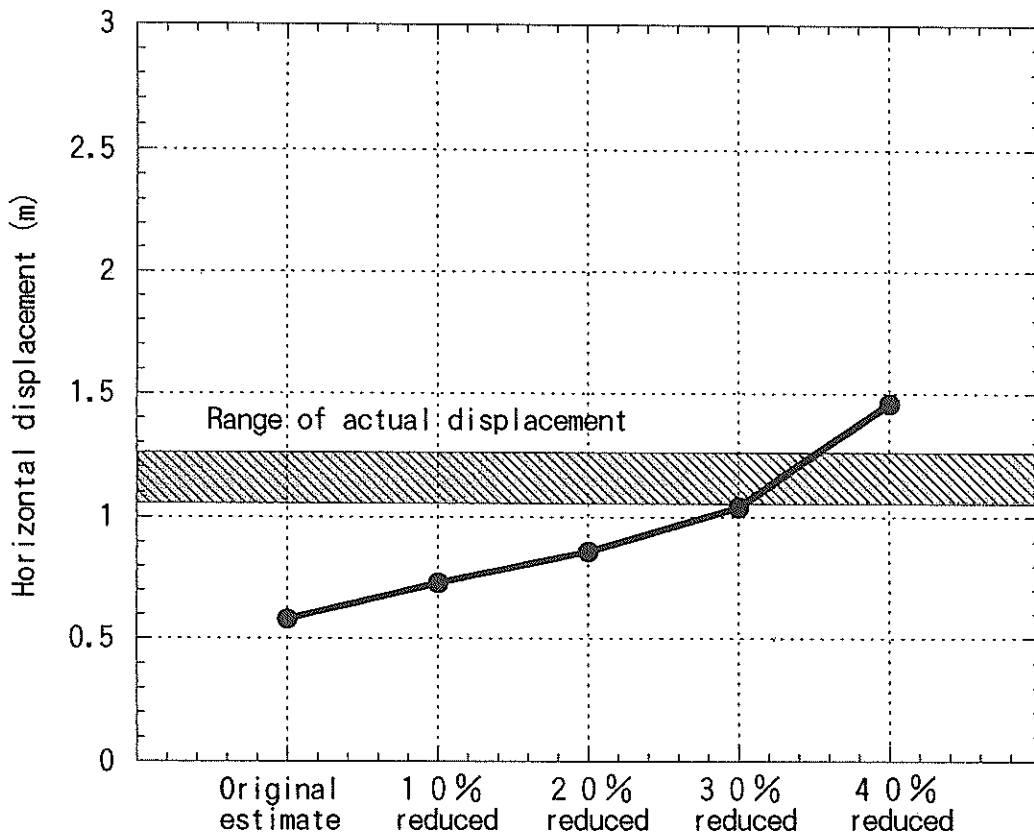


Figure 27 Horizontal displacement with reduced liquefaction resistance

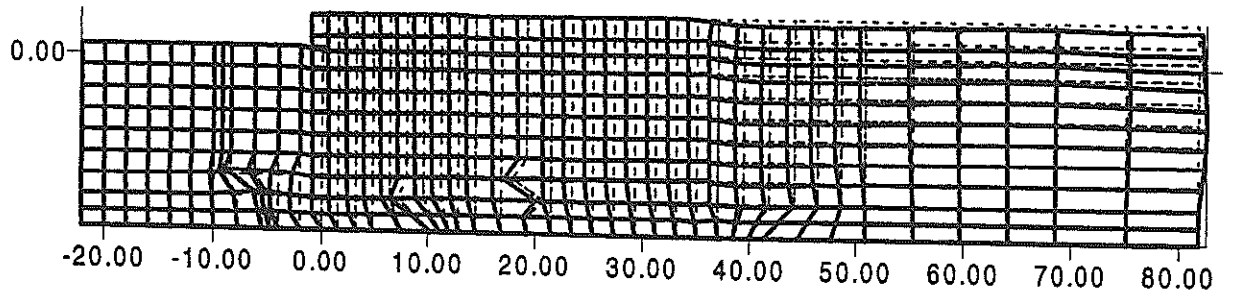


Figure 28 Computed deformation after the earthquake with 30% reduced liquefaction resistance

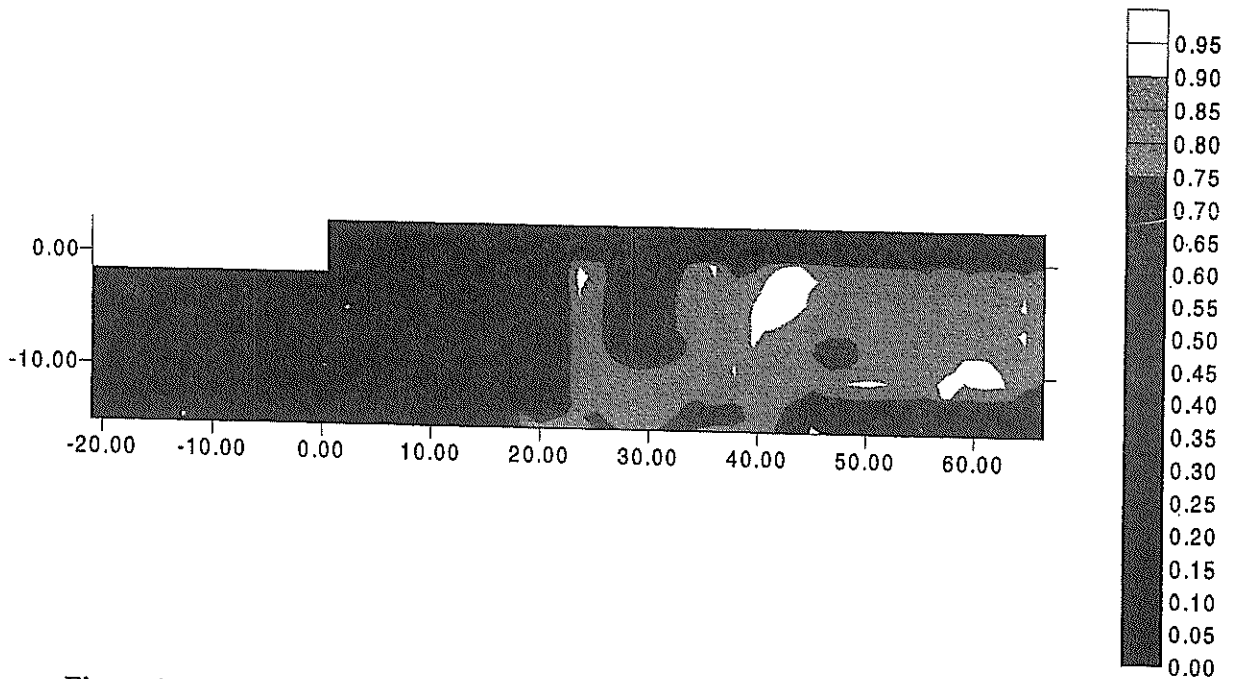


Figure 29 Computed excess pore water pressure ratio after the earthquake with 30% reduced liquefaction resistance

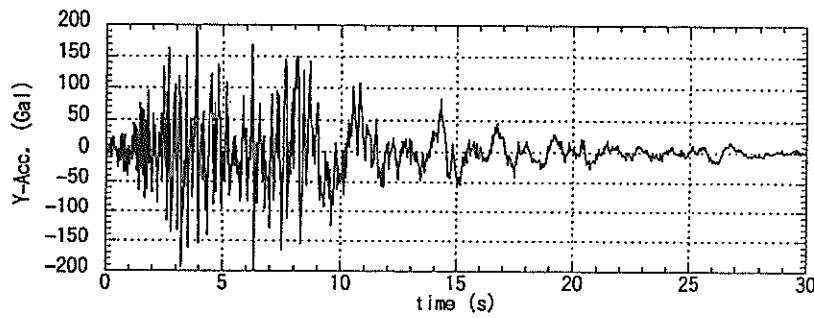
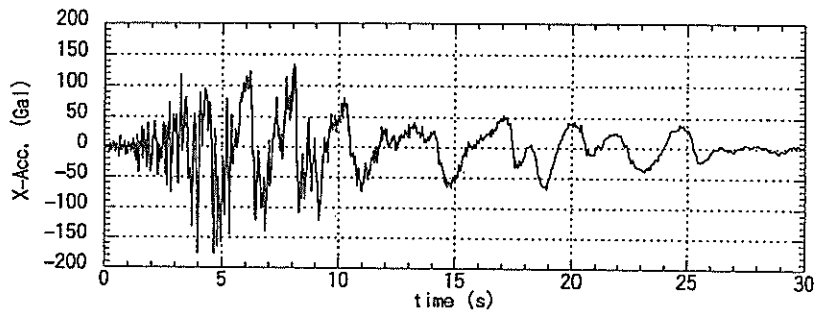


Figure 30 Computed time history of acceleration at the top of caisson, 30% reduced liquefaction resistance

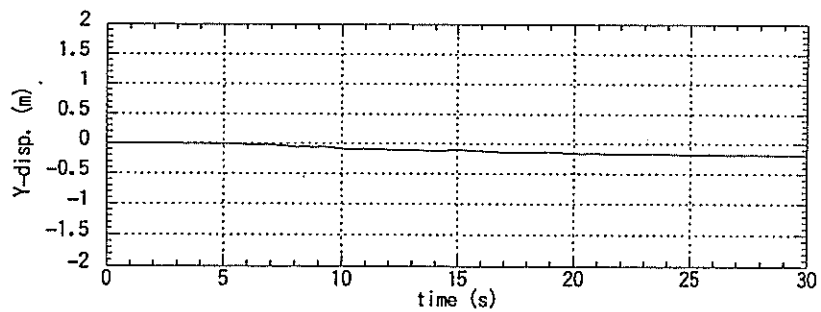
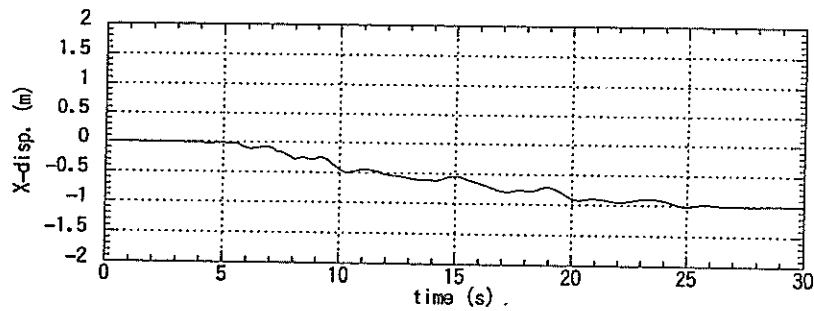


Figure 31 Computed time history of displacement at the top of caisson, 30% reduced liquefaction resistance

4.2 The effect of the existence of the old steel cellular structure

As shown in Figure 2, the caisson of the high seismic resistance quay wall is constructed in front of the steel cellular type quay wall. When the seismic performance of other quay walls is estimated based on the performance of this quay wall, the effect of the former steel cellular type quay wall should be ignored. For this reason, analyses without steel cellular elements (beam and joint elements) were performed. A parametric study of liquefaction resistance was also conducted. Computed horizontal displacement under various levels of liquefaction resistance is shown in Figure 32. Similar to Figure 27, the observed displacement is indicated with a dark hatch. The dotted line shows the displacement without the cellular structure and indicates that the displacement without the cellular structure is two times the displacement with the cellular structure. The displacement with the cellular structure is probably underestimated since the cellular structure is assumed to be rigid block. Therefore, the actual performance of the quay wall is probably somewhere in between the performance predicted with and without the cellular structure, as shown in Figure 32. The computed deformation and excess pore water pressure ratio after the earthquake for the case without the cellular structure and for 30% reduced liquefaction resistance are shown in Figures 33 and 34, respectively. Without the cellular structure, the area of settlement in the backfill rock is greater and the inclination of the caisson increases from 0.7 degrees with the cellular structure to 2.6 degrees without the cellular structure.

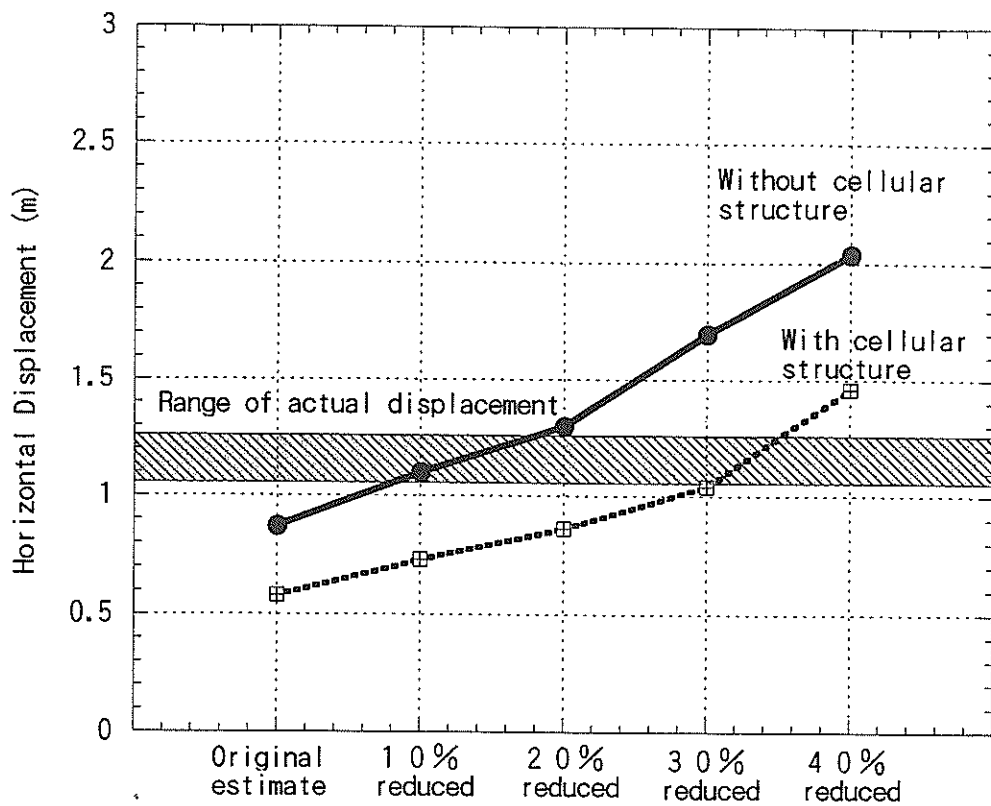


Figure 32 Computed horizontal displacement under various liquefaction resistances, with and without cellular structure

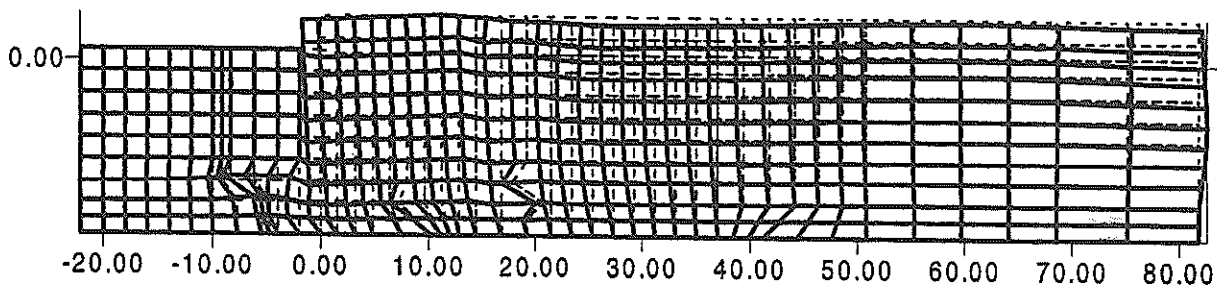


Figure 33 Computed deformation without the cellular structure, 30% reduced liquefaction resistance

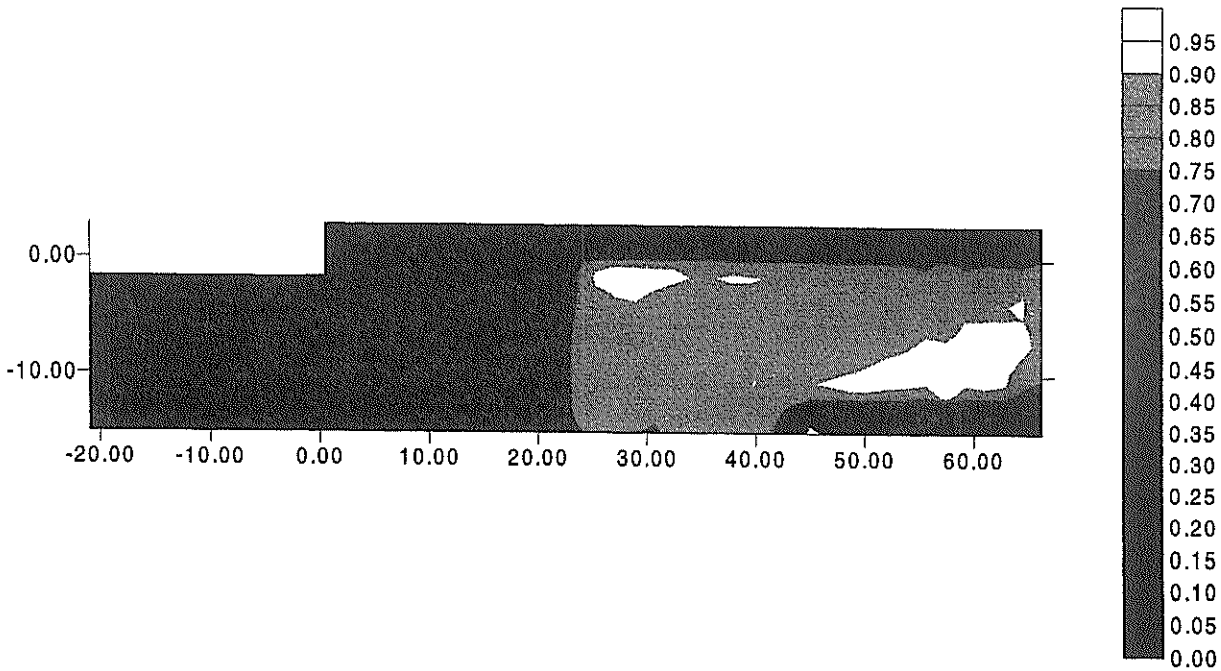


Figure 34 Computed excess pore water pressure ratio without the cellular structure, 30% reduced liquefaction resistance

4.3 The effect of ground liquefaction

Though a parametric study varying the liquefaction resistance was conducted to consider the effect of multiple directional shaking, the effect of ground liquefaction or increase in excess pore water pressure itself has not been considered. Therefore, we performed an idealized analysis using non-liquefiable soil which has the same properties as usual sand, except it shows no dilatancy. Computed acceleration and displacement time histories at the top of the caisson are shown in Figures 35 and 36, respectively. Computed residual displacement at the top of caisson is only 0.1 m. Thus, the analysis essentially predicts zero deformation. The observed deformation at Maya Wharf was mainly induced by liquefaction in both the sand replacement layer and the backfilled sand. Therefore, considering the effect of the former cellular type quay wall and the orientation of the face line of the quay wall parallel to the predominant direction of earthquake shaking, the quay wall would show no deformation if countermeasures against liquefaction were perfectly conducted before the earthquake. In other words, though the deformation of the quay walls was reduced by the presence of the cellular structure and the mismatch of the strong shaking direction, liquefaction in the soil replacement layer and behind the quay wall induced horizontal displacement of about 1 m in average.

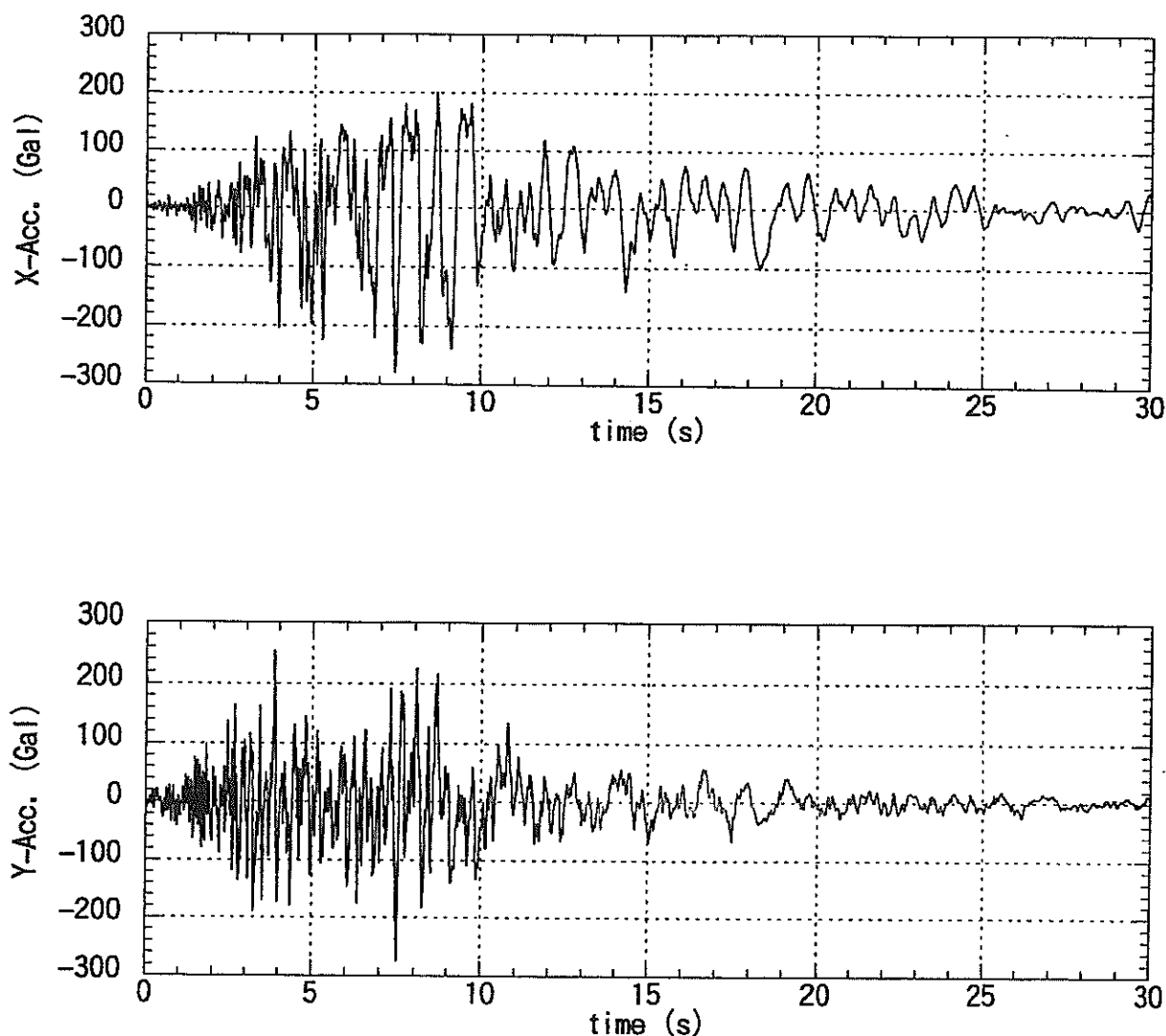


Figure 35 Computed time history of acceleration at the top of caisson considering no dilatancy of soil

5. High seismic resistant design of quay walls

5.1 Seismic performance relative to designed seismic coefficient

High seismic resistance quay walls in Maya Wharf were designed with a seismic coefficient of 0.25. The existence of the former steel cellular type quay walls behind the caissons was ignored during the seismic design. To consider the effect of high seismic resistant design, computed displacement of the high seismic resistance quay walls without the cellular structure and computed displacement of usual type quay walls are compared. The -14m type quay walls at the south end of Rokko Island designed with a seismic coefficient of 0.15 were analyzed as usual type quay walls. The details of the analyses on these quay walls were reported by Iai et al²⁾.

To consider the most severe condition, the recorded motion at Port Island in the N-S direction, maximum 544 Gal, which is close to the horizontal predominant direction of motion, was used as input ground acceleration for the analyses. The input motion is shown in Figure 37. A parametric study of input acceleration levels of 100, 200, 300, 400 and 544 Gal was conducted. For liquefaction resistance, two series of analyses using non-liquefiable soil and liquefaction resistance estimated by the in-situ freezing sampling were conducted. Here, the results of in-situ freezing sampling in Port Island were used for the high seismic resistant designed case as mentioned earlier and the

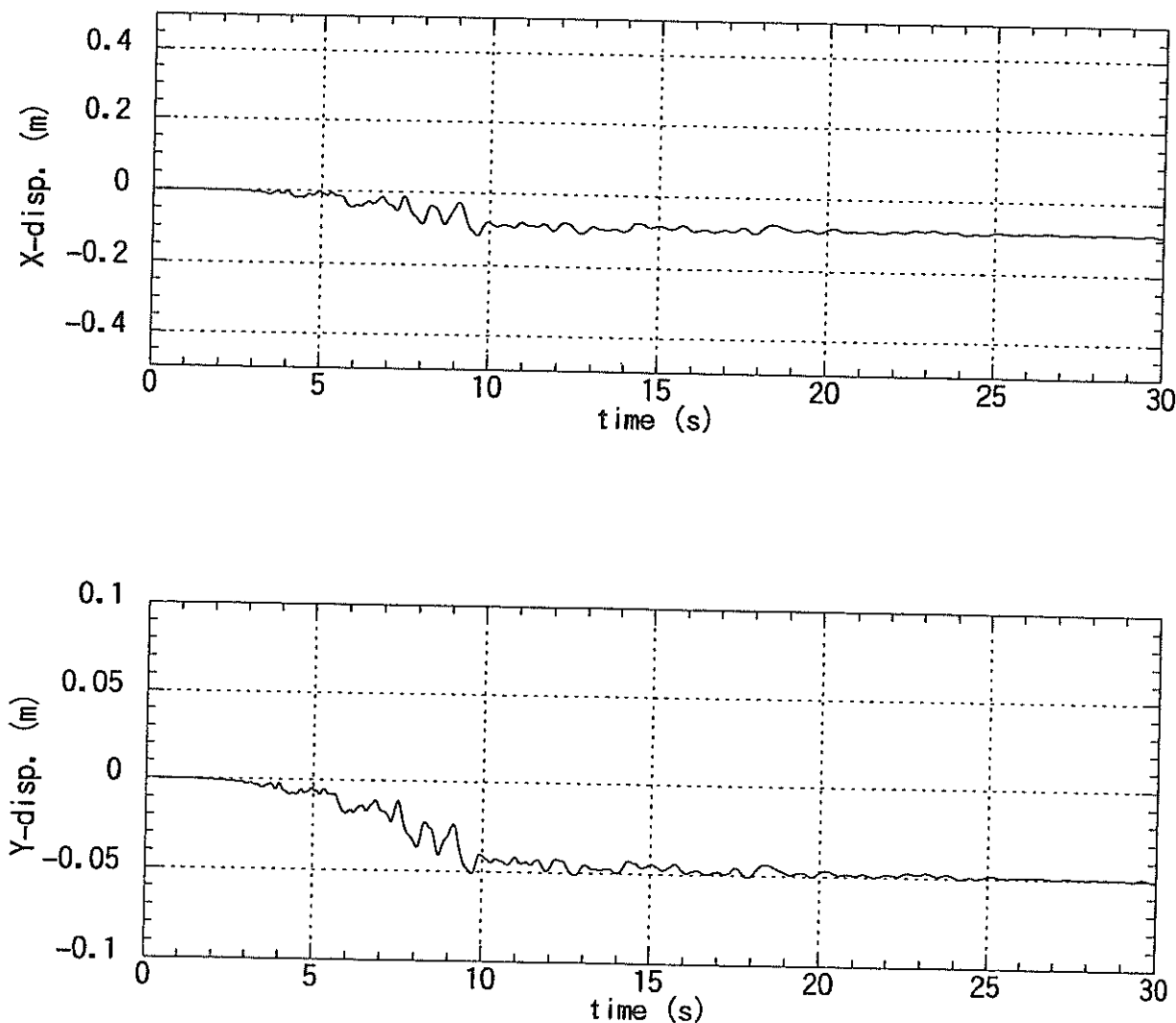


Figure 36 Computed time history of displacement at the top of caisson considering no dilatancy of soil

results of in-situ freezing sampling in Rokko Island were used for the usual quay wall case. As mentioned earlier, there is no soil improvement at the seaside clayey layer under the caisson in the high seismic resistant designed case and large deformation can be induced. Therefore, in the case with the high seismic resistance quay wall with non-liquefiable soil, we assume the soil improvement in the seaside clayey layer under the caisson was done and the same material parameters for the sand replacement layer were used. The area near the seaside basement that is assumed to be improved is shown in Figure 38.

The results of numerical parametric study are shown in Figure 39. Deformation of the high seismic resistance quay walls with no liquefaction does not increase until the maximum input acceleration exceeds 200 Gal. On the other hand, the deformation of the usual caisson type quay walls with no liquefaction increases linearly just after the maximum acceleration exceeds 200 Gal.

Discussed maximum acceleration is defined in the basement rock and there is no apparent relation with static seismic coefficient used in design. But Noda, Uwabe and Chiba presented an empirical relation between observed maximum acceleration on ground and equivalent seismic coefficient. Noda and Uwabe's empirical formulation is summarized as follows¹³⁾.

$$K_e = \frac{\alpha}{g} \quad (\alpha < 200Gal) \quad (10)$$

$$K_e = \frac{1}{3} \left(\frac{\alpha}{g} \right)^{\frac{1}{3}} \quad (\alpha \geq 200Gal) \quad (11)$$

where

- K_e : Equivalent seismic coefficient acting on quay walls
- α : Maximum acceleration at the ground surface in SMAC equivalent type acceleration
- g : Gravity acceleration

SMAC equivalent type acceleration is equivalent to the acceleration recorded by the SMAC accelerograph and it can be computed by the SMAC equivalent filter.

Therefore, the equivalent seismic coefficient can be estimated using the computed maximum acceleration at the ground surface. We used both the equivalent linear method and the effective stress analysis method to compute the maximum acceleration at the ground surface. The estimated equivalent seismic coefficients are summarized in **Figure 39** as a reference of maximum input acceleration level at the base rock. The 100 Gal acceleration level in the base rock is amplified to 110 to 130 Gal in SMAC equivalent acceleration at the ground surface and equivalent to seismic coefficient 0.11 to 0.13. It follows that the usual type quay walls designed with seismic coefficient 0.15 remain at a small deformation level for this level of acceleration. When the input acceleration level at the bedrock exceeds 200 Gal, because of the effect of non-linearity of soils, no major amplification of acceleration at the ground surface is observed. Maximum acceleration at the ground surface remains constant at about 300 Gal in SMAC equivalent acceleration when input acceleration at the bedrock exceeds 300 Gal. It means the equivalent seismic coefficient never exceeds 0.22 or 0.23 in this case, and it is difficult to discuss the equivalent seismic coefficient when the input acceleration level at the basement rock exceeds 300 Gal.

Although it is difficult to discuss the seismic coefficient and input acceleration level, the minimum acceleration level that causes deformation for a given seismic coefficient can be estimated from **Figure 39**. For example, the minimum acceleration level for the usual type quay walls designed with seismic coefficient 0.15 is about 200 Gal and for high seismic resistant type designed with a seismic coefficient of 0.25 and liquefaction countermeasures is about 400 Gal. In **Figure 39**, observed displacements of the quay walls at Rokko Island and Maya Wharf are shown, and the displacement agree with the computed deformation considering liquefaction. As mentioned earlier, we consider the orientation of the face line of high seismic resistance quay walls, and 30% reduced liquefaction resistance was used for the high seismic resistant case. Therefore, it is impossible to use input motion of 400 Gal or more, since we assume 700 Gal or more acceleration for the parallel direction of face line in this case. This is the reason the deformation with the input motion over 300 Gal are shown with dotted line in **Figure 39**.

When liquefaction countermeasures were completely done, displacement of quay walls was fairly reduced. Especially for the high seismic resistant case, the displacement is only about 30 cm for 400 Gal input and only about 90 cm for 544 Gal input. These results indicate that the effectiveness of the high seismic resistant design is increased when liquefaction countermeasures are completely conducted.

For the large input acceleration level, displacement of the usual type quay walls with liquefaction countermeasures is smaller than that of the high seismic resistance designed quay walls without liquefaction countermeasures. It can be said that liquefaction countermeasures are more effective than seismic design with a large seismic coefficient in some cases. It is necessary to conduct liquefaction countermeasures for high seismic resistance quay walls, since seismic performance of quay walls depends on both seismic coefficient and liquefaction resistance level.

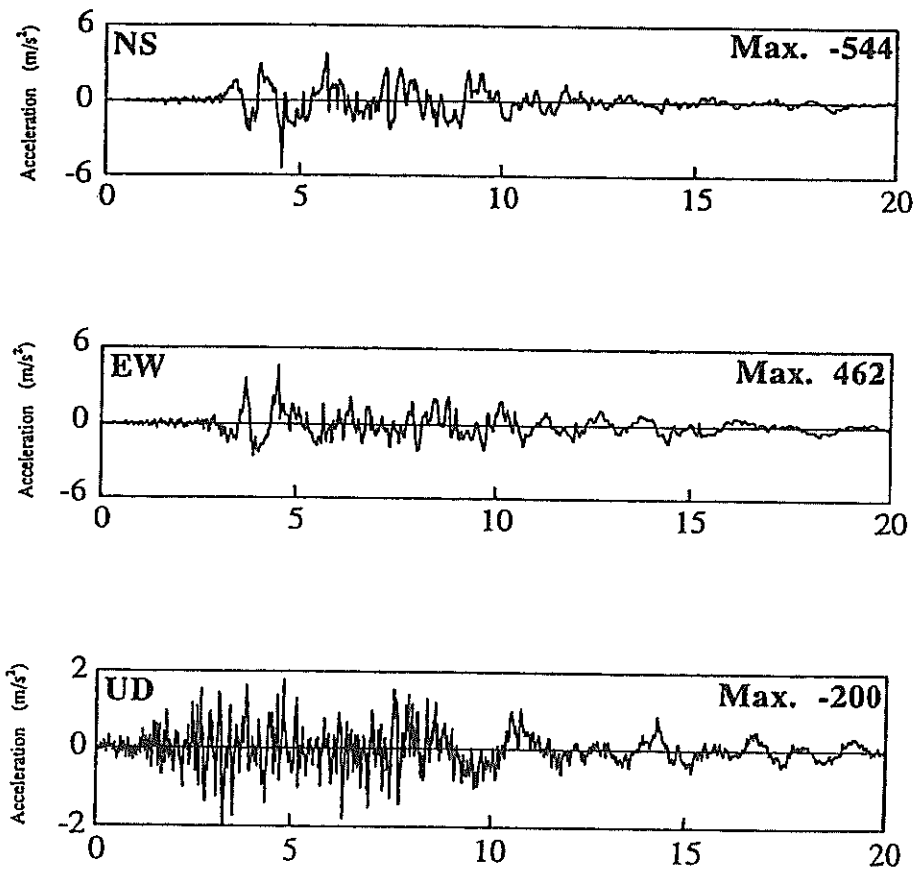


Figure 37 Input acceleration for the analyses recorded by Kobe City in Port Island at GL -32m

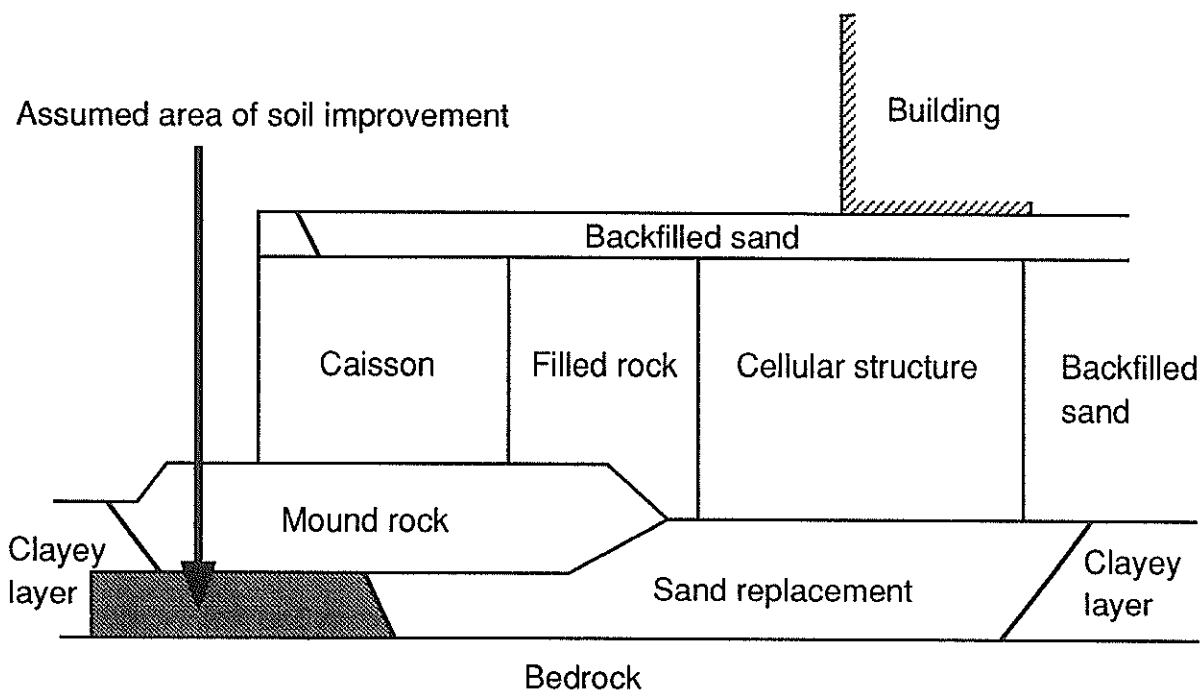


Figure 38 Assumed area of soil improvement at the seaside bottom of caisson

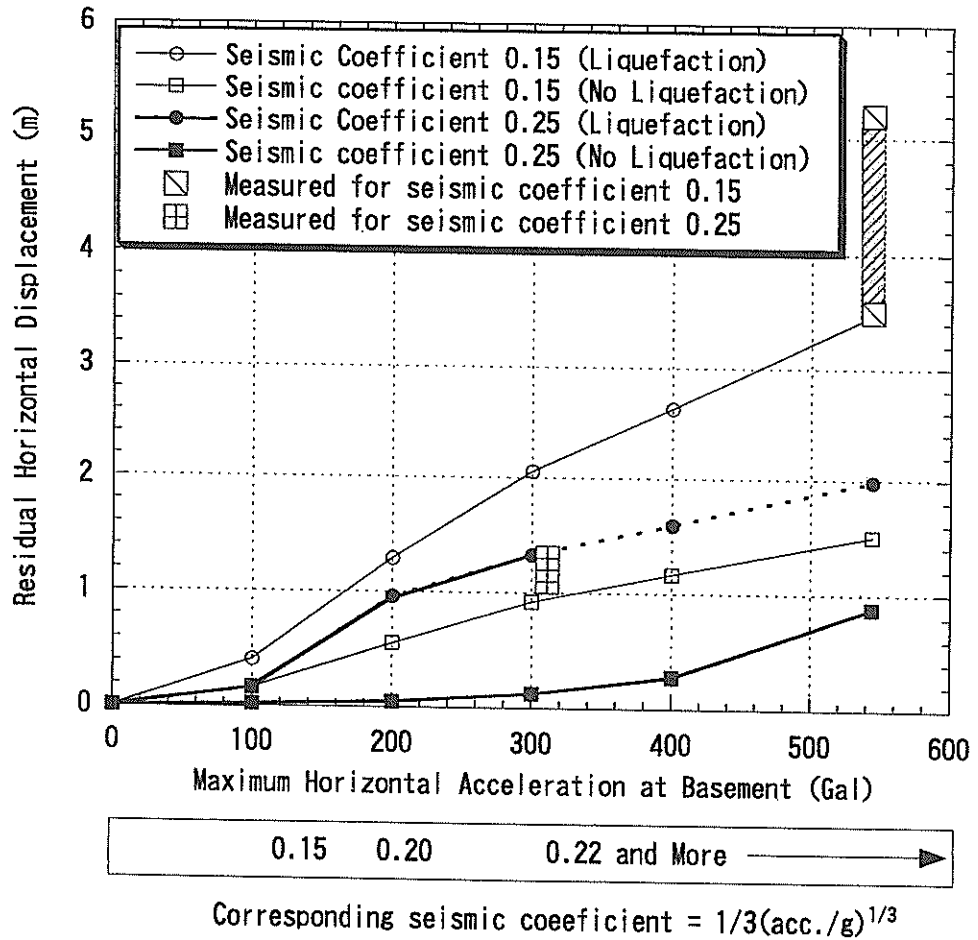


Figure 39 Horizontal displacement under various input acceleration levels

5.2 Level of improved liquefaction resistance

To consider the effect of liquefaction countermeasures, we used the idealized non-liquefiable sand for the aforementioned analyses. Since not only liquefaction resistance but also soil properties such as shear modulus might change when liquefaction countermeasures are conducted, it is necessary to consider the effect of liquefaction countermeasures themselves and the desirable level of soil improvement.

SPT N values are often used for the evaluation of soil properties including liquefaction resistance since other methods are more expensive or lack reliability. In this case, an equivalent SPT N value corrected for 0.66 kg/cm² overburden pressure is used for port structures design. Since a simplified method for parameter calibration in FLIP program using equivalent SPT N value is presented⁸⁾, we conducted the parametric study considering the level of liquefaction countermeasures using equivalent SPT N values. The results under equivalent SPT N values of 5, 10, 15, 20 and 25 are summarized in Figure 40. The high seismic resistance designed quay walls at Maya Wharf and recorded NS directional motion at Port Island with maximum acceleration of 544 Gal were used for this parametric study. If the equivalent SPT N value exceeds 20, residual horizontal displacement remains under 1.0 m which shows good seismic performance. It can be concluded that quay walls designed with a seismic coefficient of 0.25 and liquefaction countermeasures at the level of equivalent SPT N value of 20 can survive under the great earthquake motion of peak bedrock acceleration of 544 Gal.

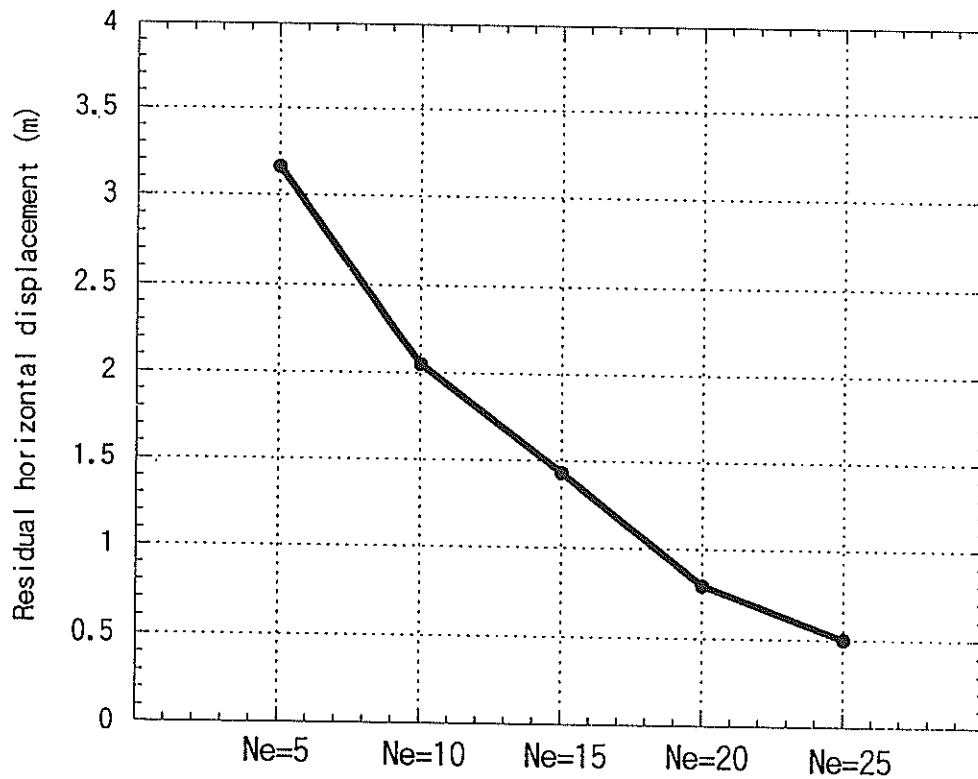


Figure 40 Horizontal displacement related to the equivalent SPT N values

6. Conclusion

Two-dimensional effective stress analyses for high seismic resistance quay walls at Maya Wharf were conducted. The performance of the quay walls is summarized as follows.

- (1) Computed deformation is smaller than observed deformation. This might be due to the effect of multidirectional shaking on liquefaction resistance, which is neglected in the two-dimensional effective stress analyses. Reducing the liquefaction resistance by 30% results in a predicted deformation that agrees with the observed deformation.
- (2) The existence of the steel cellular type quay walls behind caisson walls reduced the deformation. Without the cellular structure, the observed deformation might be amplified about two times.
- (3) The observed deformation of the high seismic resistance quay walls at Maya Wharf are mainly caused by liquefaction in the sand replacement layer and filled sand behind the quay walls. Therefore, adequate liquefaction countermeasures can limit the deformation.

In comparison with the usual type quay walls, the performance of high seismic resistance quay walls is as follows.

- (4) The minimum input acceleration required level for deformation to occur increases when the quay walls are designed with large seismic coefficients. This trend is clear when liquefaction countermeasures are conducted. The quay wall with large seismic coefficient and adequate liquefaction countermeasures have fairly good seismic performance. For example, even with a large input motion with maximum acceleration of 544 Gal, horizontal displacement at the top of the quay walls can remain under 1.0 m if liquefaction countermeasures are completely done.

(Received on September 30, 1998)

References

- 1) Inagaki, H., Iai, S., Sugano, T., Yamazaki, H., and Inatomi, T. : Performance of caisson type quay walls at Kobe port, *Special Issue of Soils and Foundations*, 1996, pp.119-136.
- 2) Iai, S., Ichii, K., Liu, H. and Morita, T. : Effective stress analyses of port structures, *Special Issue of Soils and Foundations*, 1998, Japanese Geotechnical Society.
- 3) Sugano, T., Morita, T., Mito, M., Sasaki, T. And Inagaki, H. : Case studies of caisson type quay wall damage by 1995 Hyogoken-nanbu earthquake, *Proceedings of eleventh world conference on earthquake engineering*, 1996, Acapulco, Mexico.
- 4) Sato, Y., Ichii, K., Sato, Y., Hoshino, Y., Miyata, M., Morita, T. and Iai, S. : Strong-motion earthquake records on the 1995 Hyogo-ken nanbu earthquake in port areas, *Technical note of the Port and Harbour Research Institute*, 1998, No. 907.
- 5) Iai, S., Matsunaga, Y and Kameoka, T. : Strain space plasticity model for cyclic mobility, *Soils and Foundations*, 1992, Vol. 32, No. 2, pp.1-15.
- 6) Iai, S., Matsunaga, Y. and Kameoka, T. : Analysis of cyclic behavior of anisotropically consolidated sand, *Soils and Foundations*, Vol. 32, No. 2, 1992, pp.16-20.
- 7) Zienkiewicz, O.C. : The Finite Element Method, 3rd edition, McGraw-Hill Book Co., 1977.
- 8) Morita, T., Iai, S., Liu, H., Ichii, K. And Sato, Y. : Simplified method to determine parameter of FLIP, *Technical note of the Port and Harbour Research Institute*, No. 869, 1997 (in Japanese).
- 9) Inatomi, T. et al. : Damage of port and port-related facilities by the 1995 Hyogoken-nanbu earthquake, *Technical note of the Port and Harbour Research Institute*, No. 857, 1997. (in Japanese).
- 10) Sugito, M., Sekiguchi, K., Yashima, A., Oka, F., Taguchi, Y and Kato, Y. : Correction of orientation error of borehole strong motion array records obtained during the South Hyogo Earthquake of Jan.17, 1995, *Journal of Structural Mechanics and Earthquake Engineering*, No. 531, I-34, JSCE, 1996, pp.51-63.
- 11) Yoshimi, Y. : Liquefaction of Sandy Deposit, *Gihoudo Press*, 1991, 2nd edition, pp.86(in Japanese).
- 12) Ichii, K., Iai, S. and Morita, T. : Effective stress analyses on the performance of caisson type quay walls during 1995 Hyogoken-nanbu earthquake, *Report of the Port and Harbour Research Institute*, Vol. 36, No. 2, 1997, pp.41-86 (in Japanese).
- 13) Noda, S., Uwabe, T. and Chiba, T. : Relation between seismic coefficient and ground acceleration for gravity quay wall, *Report of the Port and Harbour Research Institute*, Vol. 14, No. 4, 1975, pp.67-111 (in Japanese).